# MODELLING OF DOWNHOLE SEISMIC SOURCES I: LITERATURE REVIEW, REVIEW OF FUNDAMENTALS, IMPULSIVE POINT SOURCE IN A BOREHOLE

by

**J.A. Meredith, C. H. Cheng, and M. N. Toksöz**

**Earth Resources Laboratory**
**Department of Earth, Atmospheric, and Planetary Sciences**
**Massachusetts Institute of Technology**
**Cambridge, MA 02139**

## ABSTRACT

This paper represents the first of a two paper sequence comprising a multi-faceted introduction to the numerical and analytical modelling of seismic sources in a borehole. Part one will present a literature review and a review of the fundamental mathematical descriptions of wave propagation outside a borehole. By listing the mathematical descriptions here we can show the equivalence and interrelationships of many treatments presented in the literature. Part one will conclude with an outline of the familiar discrete wavenumber technique as applied to modelling radiation outside a borehole from a point source inside a borehole. Part two will attempt to isolate the effects of the fluid-filled borehole on the radiation of a borehole source by comparing radiation patterns for three cases: a point source in an infinite medium, a stress applied to the wall of an empty borehole (Heelan's (1953) result) and a point source in a fluid-filled borehole (Lee and Balch, 1982). Heelan's results will also be analyzed and defended against criticism of them brought by Jordan (1962) and Abo-Zena (1978).

The literature review will be thorough and will include the work done directly on modelling downhole seismic sources and the comparatively larger amount of work done on modelling sources for acoustic logging purposes which is directly applicable.

Different authors publishing work on seismic sources have made widely different symmetry assumptions ranging from no symmetry to axisymmetry to symmetry along the $z$ axis. These differences hamper the ability to directly compare results between the different treatments. Compounding the differences in symmetry are the use of different time dependencies ($e^{-i\omega t}, e^{i\omega t}$) and the use of different Hankel function or modified Bessel function strategies. Therefore, the mathematical fundamentals of wave

propagation in a borehole from the different symmetry systems are presented here in a consistent notation and are related to each other and treatments in the literature to help eliminate duplication of effort.

Finally, wave propagation outside a borehole is examined using synthetic seismograms. For the synthetic seismograms, a point source inside the borehole is used as a source and the synthetics are calculated using the discrete wavenumber method. The synthetic seismograms are measured along vertical arrays of point receivers placed outside the borehole and for lithologies of Pierre shale, Solenhofen limestone, and Berea sandstone. The method and the resulting seismograms are outlined in this paper along with a brief description of the discrete wavenumber technique.

## INTRODUCTION

Although there has been much work done on the modelling of downhole sources, most of the radiation studied has been radiation propagating inside the borehole. The description of radiation outside the borehole is important in understanding reverse VSP experiments, measurement while drilling (MWD) experiments, and crosshole tomography experiments.

The reason these technologies are being actively pursued is that reflection seismology while very robust does occasionally suffer from limitations in mature basins or for developmental purposes. This is less of a problem with 3-D reflection seismology but even then limitations arise.

The principal limitations of reflection seismology data are resolution, the near surface problem and lateral heterogeneity which are all complexly intertwined. The resolution problem is related to the type and size of traps being sought. In the continental U.S. especially, where most easily found structural traps have been found, focus is shifting to stratigraphic traps which often follow tortuous paths. The limiting factor on the resolution is the lack of frequency coverage obtainable because the near surface attenuates and scatters the high frequency energy. Another limiting factor on the bandwidth obtainable is attenuation over the large distances seismic waves travel to the target and then back up to the surface. Lateral heterogeneity makes velocity analysis complex and difficult.

Crosshole tomography is one experimental technique that is trying to address some of these problems. The principal focus of this paper will be the radiation of downhole sources as it applies to crosshole tomography. Crosshole tomography is a technique that uses two boreholes in which a source is placed in one borehole and receivers in the other. By moving sources and receivers up and down the adjacent borehole an image of the geology between the two boreholes can be reconstructed.

Tomography is a term meaning the description (graphy) of a medium by slices (tomo). Its most familiar manifestation is in the medical sciences where noninvasive x-ray slices are taken through planes of a patient. By revolving the x-ray source and receiver around the patient a CAT (computerized axial tomography) scan is produced with full azimuthal coverage. By moving the patient, any number of slices or planes perpendicular to the patient can be imaged.

Crosshole tomography is similar to medical tomography but with substantial limitations not encountered in the medical application. The primary limitation is that geophysicists cannot rotate sources and receivers around a target and thus full azimuthal coverage is impossible. With a cross hole experiment we can utilize the surface transmitted wavefield and the transmitted wavefield from the pair of boreholes, or ideally 180 degrees of azimuth. An x-ray travels in a straight line which makes reconstruction of its path particularly simple. Conversely with geologic materials, substantial and unpredictable bending of raypaths occurs complicating reconstruction of the raypath. A third limitation is that secondary arrivals such as fluid borne Stoneley waves can also contaminate our data and cannot be properly resolved through raytracing. The fourth limitation is that crosshole tomography experiments can only image one plane at a time and we are limited to the planes provided by the locations of preexistent boreholes. The final limitation is that an x-ray source because of its small dimensionality can be considered a point source which is not the case for crosshole tomography. However, crosshole tomography sources are commonly modelled as point sources.

Despite these limitations, crosshole tomography offers substantial promise. Because sources are placed down hole, the surficial sediments are avoided so scattering and attenuation are considerably reduced and higher frequencies can be utilized. Up to 15 fold increases in frequency bandwidth are theoretically obtainable. Additionally, the sources and receivers are closer to the target and removed from cultural noise. However, even with these recording and frequency advantages, the full waveform is not used. Instead, present processing techniques rely on inverting first-break arrival times from compressional waves. Ray methods specifying point sources and receivers are used to generate the forward models for the inversion process. An important aspect of the ray methods is that the borehole is not considered in the point source representation. A good paper detailing these ray based techniques is by Wu and Toksöz (1987) which complements a good paper on laboratory observations by Lo et al. (1988).

## Inadequacy of the Point Source in an Infinite Medium Representation

A primary reason for not utilizing the full waveform recorded in crosshole experiments is the inadequacy of the point source representation. The point source representation used is that of a point source in an infinite elastic medium with no borehole, no fluid and no casing present. There are many reasons why a seismic source in a borehole

is inadequately represented by this kind of representation. The most obvious is the presence of the fluid-filled borehole in which the source is fired and the received waveforms are recorded. In traversing a fluid-filled to a solid medium, strong interface or guided waves are generated. The most energetic type of guided wave is the Stoneley or "Tube" wave. The tube wave travels up and down the borehole at a velocity less than fluid velocity. For some source configurations, much of the energy expended from downhole sources is seen as tube wave arrivals.

The past justification for ignoring borehole effects was that in the far field the distorting effects of the borehole were negligible and the guided waves would attenuate exponentially away from the originating borehole. A rule of thumb was developed that the borehole effects would be negligible if the diameter of the borehole was 30 times less than the dominant wavelength. This "low frequency" assumption has lost its validity with the high frequency sources being utilized and developed today. For instance, one kilohertz source frequencies generate wavelengths, at typical 2-5 km/sec velocities, of only 2-5 meters. This is typically only 10 times greater than the borehole diameter and thus substantial distortion can occur.

A second limitation in the point source representation has been that the wavefronts incident on the receiver borehole also generate secondary guided waves. Tube waves generated in the receiver borehole distort primary arrivals as well. Crosshole tomography surveys are often performed in cased boreholes. A string of steel casing provides a stiffness surrounding the borehole that is difficult to ignore and a major contributing factor to tube wave generation both in the receiver and source borehole. Therefore, the low-frequency assumptions have also lost their validity in practice because of the dominance of tube waves on the recorded waveforms in the receiver borehole.

A final limitation is that for various reasons of safety and repeatability, downhole sources such as vibrators and piston mechanisms are being developed which do not abide by the point source representation either spatially or temporally. We will begin to address this omission in the modelling of downhole seismic sources by providing a thorough description of the physical modelling of downhole sources. But first a review of the literature leading up to the present day description of downhole sources for crosshole tomography purposes.

## LITERATURE REVIEW

Many attempts to look at the propagation of sources from empty or fluid-filled cylindrical cavities were made in the fields of vertical seismic profiling and sonic well logging. Most of the crosshole source theory has been as extensions of work in sonic well logging and most of the experimental technique has come from developments in VSP and reverse VSP technology. Therefore pertinent sonic well-logging and VSP literature will

be detailed here along with work intended for downhole source description.

Heelan's results (1952, 1953a,b) are very frequently referenced in the source description problem because his was one of the first treatments of radiation from boreholes. Heelan modelled explosive charges as sources radiating from a finite length of an infinite cylindrical cavity embedded in an infinite elastic medium. He solved two independent problems: that arising from the point dislocation of stress in the radial and/or axial (tangential) direction applied to the borehole wall and that due to a point torque or torsional source axisymmetrically applied to a borehole. Heelan's results and radiation patterns have been widely influential. His papers were credited with demonstrating the generation of shear waves by artificial sources in a borehole; at the time this was a fundamentally surprising result. Despite their wide citation, his mathematical development has been criticized principally by Jordan (1962), Hazebroek (1966) and Abo-Zena (1977), a topic to be addressed in paper two.

Biot (1952) in an axisymmetric treatment of wave propagation along a borehole developed a Rayleigh wave type period equation for the empty borehole, Biot's equation 2.16, and analogous period equations for the reflected conical (pseudo-Rayleigh) and Stoneley (tube) waves, Biot's equations 3.13 and 3.14 respectively, in a fluid-filled borehole. Biot used these period equations for calculation of phase velocity and group velocity dispersion curves. He showed that with axisymmetry only two potentials were needed to properly describe the resulting behavior. By taking the low frequency limit of his Stoneley wave period equation, Biot developed an asymptotic relation now known as the tube wave equation. Biot (1956) published a pair of influential articles on wave propagation in porous media, what has since become known as Biot theory. However, he did not relate Biot theory to his fundamental study of wave propagation along a borehole; that awaited the work of Rosenbaum to be discussed later.

J.E. White has been a prolific author in the field of source description theory. White (1953) first developed a strategy for modelling tube wave generation from an incident plane wave on a fluid-filled borehole by decoupling the fluid contribution from that of an empty cylinder and then recoupling them through the use of boundary conditions. White (1960) investigated the use of the reciprocity theorem for determining radiation emanating from a radial stress on a borehole, and obtained relations equivalent to Heelan's (1953a) using results from the 1953 White paper . White (1962) rederived Biot's equations and showed for imaginary arguments the Bessel functions in Biot's developments were in fact real and not imaginary. This realization was important because of the difficulty in calculating Bessel functions of complex argument at that time. White and Sengbush (1963) did a field investigation of wave propagation in a generally homogeneous medium, the Pierre shale of Colorado. White and Sengbush devoted attention to tube wave propagation and were the first to discover the substantial difference in radiation from a fluid-filled borehole compared to that from an empty borehole as developed by Heelan (1953). White and Sengbush (1963) showed

the large effects of tube waves on the resulting waveforms. White (1965) in his first book derived the tube wave equation of Biot (1952) and reproduced the theory for axisymmetric wave guides cited in Biot (1952), White (1962), and White (1960). White and Zechman (1968) were the first to begin calculations for non-axisymmetric modes of propagation. In his second book, White (1983), updates his important treatments and includes the development for flexural waves and general non-axisymmetric wave propagation presented in White and Zechman (1968).

Peterson (1974) calculated the full wavefield and the displacement-potential relations both inside and outside the borehole assuming axisymmetry. Rosenbaum (1974) calculated synthetic seismograms using Biot theory (Biot, 1956a,b) for porous media which was one of the most important early papers including numerical results. An important conclusion made by Rosenbaum was that tube waves are attenuated with increasing permeability.

Roever et al. (1974) calculated the full wavefield inside the borehole as a complete sum of characteristic modes. Modes were indexed by circumferential index number $l$ and radial mode number $n$. The fundamental mode $l = 0$ is the limiting axisymmetric case in this formulation and corresponds to the source being on the borehole axis at $r = 0$. Roever et al. set up the formalism for calculating the propagation for sources off axis. For determining properties of individual events they advocated high frequency asymptotic ray theory. In the limits of high frequency, their modal developments became branch-line integrals. The tube wave was recognized in this paper as both the zero frequency limit of the dispersion equation and the sum of two integrals of different Airy functions. In this paper, Roever et al. documented a 90° phase shift each time a wave is totally reflected at the borehole axis. Roever et al. also developed the empirical relation that the shear head wave decays as $\frac{1}{z^2}$ and the compressional head wave as $\frac{1}{z \log^2 z}$ where $z$ is the distance along the borehole axis.

Abo-Zena (1977) , like Heelan (1953), investigated the radiation from a stress applied to a finite length of an infinitely long cavity in an infinite elastic medium. Abo-Zena showed that Heelan's work (1953) depended on many "unjustifiable" assumptions but yet as pointed out by White (1983) the far-field relations he developed were equivalent. Abo-Zena did however develop the theory for a non-uniform source, with Heelan's result of a steady force being a specific example. He used Laplace transform theory instead of Fourier transform theory to do so. His criticisms of Heelan's work will be addressed in the second paper (part two).

Greenfield (1978) calculated the far-field wavefield emanating from a point-force perpendicular to an empty cavity's axis. This study was carried out while investigating methods of locating distress signals from trapped miners. His treatment was completely general and assumed no symmetry. It led to development of a Fourier-Bessel expansion

involving an infinite summation and a double integral. Therefore, he evaluated the radiation patterns in the far field so well known asymptotic relations and steepest descent techniques could be invoked to simplify the computation.

Papers by Tsang and Kong (1979) and Tsang and Rader (1979) were influential in modelling radiation from point sources for sonic logging purposes. First using Simpson's rule a double integral over $k_z$ and $\omega$ was evaluated yielding the complete wavefield. The integral over $\omega$ is lifted off the real $\omega$ axis to avoid singularities and this method is known as real axis integration. Secondly they calculated the compressional head wave contribution using a steepest descent path that surrounded the compressional branch cut and evaluated the resulting integrals using Gauss-Laguerre quadrature. They then calculated the contribution from the shear head wave branch cut and the pseudo-Rayleigh pole by having the steepest descent path surround both the branch cut and the pseudo-Rayleigh pole. This technique works even if the pseudo-Rayleigh pole has crossed into the lower Riemann sheet below the cut-off frequency. They then evaluated the enclosed pseudo-Rayleigh pole by the residue theorem. These branch cut techniques reduced the computation requirements by a factor of 50.

Cheng and Toksöz (1981) reformulated the result of Tsang and Rader (1979) and applied the technique of discrete wavenumber integration (Bouchon and Aki, 1977; Bouchon, 1981) to the derivation of this problem and calculation of synthetic microseismograms. The discretization scheme they applied is an application of the method suggested in White and Zechman (1968). Like Rosenbaum (1974) and Tsang and Rader (1979), Cheng and Toksöz used complex velocities in their calculations to both lift poles off the real axis and allow the introduction of attenuation. This paper was the first to point out the effects of leaky compressional modes in a borehole embedded in a soft sediment medium. An important contribution of this paper was the comparison of calculated waveforms to actual waveforms recorded in wells that showed the theory was substantially accurate. Finally in this paper, Cheng and Toksöz also modelled the effect of the rigid tool as a shift in frequency content.

Fehler and Pearson (1981,1984) derived expressions for radiation from a borehole by considering a source as being in an infinite elastic medium and calculating a moment tensor solution. In doing so they also derived the familiar four-leaved rose radiation pattern for shear waves as Heelan did. Fehler and Pearson also applied attenuation corrections to their results. They only showed results from one lithology and results were scaled to "source dependent constants". Fehler and Pearson showed some experimental data from the Hot Dry Rock Geothermal Reservoir Project which adds some credence to the four-leaved rose pattern for $Sv$ wave propagation.

Schoenberg et al. (1981) calculated the full wavefield similar to Peterson (1974) for the axisymmetric case and developed the solution both inside and outside the borehole. In this broad paper they also investigated the use of maximum likelihood array processing techniques for extracting velocities and the effects of radial layering.

Lee and Balch (1982) published a very important paper on seismic wave radiation. In this paper, as in Peterson (1974) and Schoenberg et al. (1981), the exact solution from an inpulsive point dilatational source located in the center of an axisymmetric borehole is developed. They also develop the exact solution for a radial stress source acting on the axis of a borehole and far field radiation pattern for both cases. Lee and Balch compare their results to Heelan's and briefly show the importance of the fluid and the effect of Poisson's ratio on the radiation. Another important contribution was to show the existence of a tube wave pole governing the radiation outside the borehole in the far field.

Lee et al. (1984) and Balch and Lee (1984), described radiation from an air gun placed downhole and concluded that the primary radiation agreed well with predictions. However, they found secondary radiations due to tube waves reflecting off the bottom of the hole which were more energetic than the primary arrivals. They also experimentally confirmed Heelan's results that shear wave arrivals are generated although their borehole was fluid-filled.

Tubman (1984) and Tubman et al. (1984, 1986), like Schoenberg et al. (1981), investigated the effect of radial layering. But Tubman et al. developed the Thomson-Haskell formalism for the borehole environment and calculated waveforms and resulting velocities generated from the waveforms.

Lee (1985a,1986) formulates the source radiation problem for an arbitrary source. He assumes propagation in a medium with no symmetry like Greenfield (1978). Lee found that in the far field the presence of the fluid does not affect the radiation from torsional sources. Lee (1985b,1987) uses the reciprocity theorem (White, 1960) to calculate the wavefield due to a plane wave incident on a borehole but does not uncouple the fluid-cavity solution as White had done.

Strictly numerical strategies have been pursued by Bhasavanija et al. (1982), and Bhasavanija (1983) with finite difference modelling of the wave train inside a borehole. Pardo et al. (1984) and Stephen et al. (1985) substantially improved Bhasavanija's presentation and showed finite difference "snapshots" of the field both inside and outside the borehole. Stephen et al. (1985) introduced horizontal layering and boundaries.

Investigation of sources other than point sources began in earnest after the introduction of a dipole source shear wave logging tool (Kitsunezaki, 1980) . Developments of multipole sources have been pursued by Kurkjian and Chang (1986 — acoustic case), Kurkjian (1986) , Winbow (1985), Baker and Winbow (1985), and Kurkjian (1985) . However the use of multipole sources for crosshole experiments is just now being investigated.

Tube wave studies have been done for generating sources both inside (Beydoun, 1982; Cheng and Toksöz, 1984; Tang and Cheng, 1989) the borehole for well logging

studies and outside the borehole for VSP studies ( Beydoun et al., 1984; Cheng and Toksöz, 1984; Cicerone et al., 1988) The importance of tube waves and their contaminating influence on crosshole data was discussed by Lee et al. (1984).

Schoenberg (1986) calculated the wavefield incident on a borehole due to the passage of a low frequency plane wave exactly. He then applied a Taylor's series like expansion of the exact solution and showed given a low frequency assumption that the borehole did distort the waveforms. This was the first treatment of wave propagation incident on a borehole that did not use the reciprocity theorem.

Siggins and Stokes (1987) and Siggins (1989) address a problem similar to that of Greenfield with theoretical, numerical and experimental work. They looked at propagation surrounding an underground tunnel due to the excitation of a line force along the tunnel wall. Experimentation was done inside a mine and showed the presence of a substantial shadow zone. Their theoretical work was an extension of Viktorov's calculations for concave cylinders (Viktorov, 1958) and verified the existence of a shadow zone. The finite element results were carried up to 11 diameters outside the borehole.

Design of crosshole sources has become a topic of recent interest including a paper by Paulsson et al. (1988) describing a downhole vibrator, a paper by Owen et al. (1988) describing an arc discharge impulsive source, and a paper by Kennedy et al. (1988) describing a source that excites programmed resonances in a fluid-filled borehole. Source development work is ongoing.

## Outline of Paper

As the preceding literature review showed, there has been substantial development of source theory studied through radiation inside the borehole. Only a few papers, however, have addressed the problems of radiation outside the borehole. The papers that have addressed propagation outside the borehole (Heelan, 1952, 1953a; Lee, 1982, 1986; Kurkjian, 1986) have not been fully reconciled with experimental results (White and Sengbush, 1953; Paulsson et al., 1988). The point source radiation patterns determined from such theoretical developments are substantially different and different from those expected of point sources in an infinite medium. Because of the scarcity of results, papers with incomplete treatments of the problem are frequently referenced.

The theoretical developments from this paper will be in cylindrical coordinates. Because there are up to five types of symmetry systems frequently used with wave propagation in cylindrical coordinates in the literature, a pressing need is to properly define how developments in these different symmetry systems are related. Unfortunately, the relations are far from clear but the later section on wave equation relationships in this paper should make these interrelationships clear.

As mentioned previously, there have been very few developments of looking at wave propagation outside a fluid-filled borehole. One of the glaring inadequacies of the few developments to date has been the low frequency, far field assumptions made and the lack of waveforms for illustration. Using the technique of discrete wavenumber integration, (White and Zechman, 1968; Bouchon and Aki, 1977; Bouchon, 1981; Cheng and Toksöz, 1981) we will calculate far field displacement fields, waveforms, for axisymmetric boreholes to show near and far field effects.

Appendices will include a description of the discrete wavenumber technique and programming considerations.

## WAVE EQUATION RELATIONSHIPS IN CYLINDRICAL COORDINATES

### Background

In a cylindrical coordinate system $(r, \theta, z)$ there are four different symmetries that may be assumed: no symmetry; symmetry in $\theta$; symmetry in $z$; and a degenerate case, symmetry in $r$.

This section describes the relationship between displacement potential, wave equation, and stress-strain relations for the most general case where no symmetry assumptions are made. The same relationships are also described for the three instances in which azimuthal symmetry (axisymmetry, symmetry with respect to $\theta$) and the one case in which symmetry along the $z$ axis is assumed. Since all five of these strategies are commonly used in solving downhole source radiation problems and will be used throughout this thesis, defining their interrelationships in this section is highly desirable. The second half of this section will demonstrate how the wave equations are solved for each symmetry strategy in terms of Bessel functions and exponentials using the method of separation of variables.

The first representation is the most general, assumes no symmetry and can be considered the parent representation. We can represent the displacement field by three displacement potentials $\phi, \psi$, and $\chi$ corresponding to a longitudinal $\phi$ and two transverse waves $\psi, \chi$. One of the transverse waves is polarized vertically to the longitudinal motion ($Sv$) and the other horizontally ($Sh$). There is complete coupling between $P$-$SV$ and $Sh$ motion for this case. When a symmetry strategy is assumed, uncoupling will occur. A limiting case of this first representation is that of flexural wave propagation in which displacement is governed by functions of $\theta$ to the first power only.

The second representation assumes axisymmetry and the propagation of two kinds of waves governed by a shear wave velocity $Sv$ ($\psi$ potential) and compressional wave

velocity $P$ ($\phi$ potential). This second representation recodifies $\psi$ to simplify the algebra and boundary conditions and is very frequently found in the geophysics literature. When use is made of this recoded potential $\psi$, we will use the prime $'$ symbol to denote the transformation, $\psi'$.

The third case is equivalent to the second except the scalar potential $\psi$ is not recoded and is found in a few important references in the geophysics literature and also that of more general physics and mechanics. The fourth representation can be considered an "acoustic" case where one assumes torsional ($Sh$) motion and calculates the displacement potential $\chi$ exclusively. The final representation is commonly encountered with line source problems where symmetry in the $z$ axis is assumed and the displacement potentials $\phi, \chi$ are used.

The existence of these five representations although fundamentally related is often a source of considerable confusion to the uninitated when working with elastic wave propagation in cylindrical coordinates. Many papers assume a symmetry system without relating their developments to similar developments in other papers formulated in a diffferent symmetry system. It thus becomes difficult to reconcile the disparate developments. For instance, representation strategy two, an axisymmetric case, seems to produce a new type of cylindrical wave for $Sv$ governed by a new Bessel function governed by the recoded scalar potential $\psi'$. Although it can be clear by context which displacement potential and which wave equation relationships are being used, the purpose of this chapter is to concretely define the interrelationships between each strategy.

## Fundamental differential identities in cylindrical coordinates

The reader is familiar with the curl, divergence, gradient and Laplacian operators and their properties in Cartesian coordinates; they are presented here in cylindrical coordinates because of their fundamental importance to the discussion that follows. These relations can be found in any handbook on vector calculus (Schey, 1973). For an arbitrary vector field the symbol $\vec{K}(r,\theta,z)$ will be used and for an arbitrary scalar field the symbol $A(r,\theta,z)$ will be used.

Divergence: Operates on vector field $\vec{K}$ and yields a scalar field

$$\nabla \cdot \vec{K} = \frac{1}{r}\frac{\partial (rK_r)}{\partial r} + \frac{1}{r}\frac{\partial K_\theta}{\partial \theta} + \frac{\partial K_z}{\partial z} \tag{1}$$

Gradient: Operates on a scalar field $A$ and yields a vector field

$$\nabla A = \hat{e}_r \frac{\partial A}{\partial r} + \hat{e}_\theta \frac{1}{r}\frac{\partial A}{\partial \theta} + \hat{e}_z \frac{\partial A}{\partial z} \tag{2}$$

Curl: operates on vector field $\vec{K}$ and yields a vector field

$$\nabla \times \vec{K} = \hat{e}_r\left(\frac{1}{r}\frac{\partial K_z}{\partial \theta} - \frac{\partial K_\theta}{\partial z}\right) + \hat{e}_\theta\left(\frac{\partial K_r}{\partial z} - \frac{\partial K_z}{\partial r}\right) + \hat{e}_z\left(\frac{1}{r}\frac{\partial (rK_\theta)}{\partial r} - \frac{1}{r}\frac{\partial K_r}{\partial \theta}\right) \tag{3}$$

Laplacian: operates on scalar field $A$ and yields a scalar field

$$\nabla^2 A = \frac{1}{r}\frac{\partial}{\partial r}\left(r\frac{\partial A}{\partial r}\right) + \frac{1}{r^2}\frac{\partial^2 A}{\partial \theta^2} + \frac{\partial^2 A}{\partial z^2} \tag{4}$$

### Differential identities for modified Bessel functions

Modified Bessel functions $(K_{\{0,1\}}, I_{\{0,1\}})$ will be used throughout this thesis. Derivatives of these Bessel functions will be introduced through boundary conditions in subsequent chapters. The differential identities for these modified Bessel functions are as follows (Abramowitz and Stegun, 1964, Eq. 9.6.27,.28) assuming the variable $k$, i.e., a wavenumber, is independent of $r$

$$\begin{aligned}
\frac{\partial I_0(kr)}{\partial r} &= kI_1(kr) \\
\frac{\partial K_0(kr)}{\partial r} &= -kK_1(kr) \\
\frac{\partial I_1(kr)}{\partial r} &= k\left[I_0(kr) - \frac{I_1(kr)}{kr}\right] \\
\frac{\partial K_1(kr)}{\partial r} &= -k\left[K_0(kr) + \frac{K_1(kr)}{kr}\right]
\end{aligned} \tag{5}$$

## Displacement potential and wave equation relationships for various symmetries

### Strategy 1 - no symmetry assumptions

An arbitrary displacement field $\vec{U}$ can be represented in terms of the displacement potentials $\phi, \psi, \chi$. In the literature this strategy has been adopted by White and Zechman (1968) for flexural waves, White and Tongtaow (1981) for describing wave motion inside a borehole propagating through a transversely isotropic medium and Greenfield (1978), Lee (1986), and Schoenberg (1986) for describing radiation emanating from a

borehole and incident on a borehole. The displacement field and the displacement potentials are related by the Helmholtz representation or theorem (White and Zechman, 1968; Malvern, 1969, pg. 548; Aki and Richards, 1980, Box 6.5) as follows assuming $\vec{U}$ is continuously differentiable.

$$\vec{U} = \nabla\phi + \nabla \times \vec{K} \tag{6}$$

This is the sum of an irrotational scalar field, $\phi$, and a solenoidal (equivoluminal) vector field, $\vec{K}$. $\vec{K}$ can be further decomposed into two scalar potentials $\psi$ and $\chi$ (Morse and Feshbach, 1953, Part II, pg. 1762–1767; White and Zechman, 1968, pg. 55–56; Miklowitz, 1978, pg. 58–62; Schoenberg et al., 1981) representing respectively $Sv$ and $Sh$ waves both travelling at the shear wave velocity. The decomposition is

$$\vec{K} = \chi\hat{e}_z + \nabla \times (\psi\hat{e}_z) \tag{7}$$

or writing in terms of coordinates

$$\vec{K} = (\frac{1}{r}\frac{\partial\psi}{\partial\theta}, \frac{-\partial\psi}{\partial r}, \chi) \tag{8}$$

which yields the following for the cross product

$$\begin{aligned} \nabla \times \vec{K} \;=\; & \hat{e}_r(\frac{\partial^2\psi}{\partial r\partial z} + \frac{1}{r}\frac{\partial\chi}{\partial\theta}) + \hat{e}_\theta(\frac{1}{r}\frac{\partial^2\psi}{\partial\theta\partial z} - \frac{\partial\chi}{\partial r}) + \\ & \hat{e}_z(-\frac{1}{r}\frac{\partial}{\partial r}\left(r\frac{\partial\psi}{\partial r}\right) - \frac{1}{r^2}\frac{\partial^2\psi}{\partial\theta^2}) \end{aligned} \tag{9}$$

Like Cartesian coordinates, to uncouple $P$-$Sv$ and $Sh$ motion a gauge condition $\nabla \cdot \vec{K} = 0$ must be satisfied. For the gauge condition to be satisfied, the Neumann condition $\nabla \cdot \vec{K} = \frac{\partial\chi}{\partial z} = 0$ must be true. This is not necessarily true, and in general $P$-$Sv$ and $Sh$ motion are completely coupled if no symmetry is assumed (Pilant, 1979). Adding $\nabla\phi$ and the cross product $\nabla \times \vec{K}$ (Eq. 9) using the Helmholtz representation, (Eq. 6) the displacement potential relations are (Miklowitz, 1978, pg. 216; Tongtaow, 1982, pg. 13; Pao and Mow, 1971, pg. 219 (the roles of $\psi, \chi$ are reversed in Pao and Mow's equations from that presented here)).

$$U_r \;=\; \frac{\partial\phi}{\partial r} + \frac{\partial^2\psi}{\partial r\partial z} + \frac{1}{r}\frac{\partial\chi}{\partial\theta} \tag{10}$$

$$U_\theta \;=\; \frac{1}{r}\frac{\partial\phi}{\partial\theta} + \frac{1}{r}\frac{\partial^2\psi}{\partial\theta\partial z} - \frac{\partial\chi}{\partial r}$$

$$U_z = \frac{\partial \phi}{\partial z} - \frac{1}{r}\frac{\partial}{\partial r}\left(r\frac{\partial \psi}{\partial r}\right) - \frac{1}{r^2}\frac{\partial^2 \psi}{\partial \theta^2}$$

For infinitesimal strain, the strains in cylindrical coordinates can be calculated from the formulas for curvilinear coordinate systems as presented in Love (1927). The curvilinear coefficients are $h_r = 1, h_\theta = r, h_z = 1$. In terms of displacement these strains are (Love, 1927, pg. 56; Miklowitz, 1978, pg. 217; White, 1983, pg. 163)

$$\varepsilon_r = \frac{\partial U_r}{\partial r} \quad \varepsilon_\theta = \frac{1}{r}\left(\frac{\partial U_\theta}{\partial \theta} + U_r\right) \quad \varepsilon_z = \frac{\partial U_z}{\partial z} \tag{11}$$
$$\varepsilon_{r\theta} = \frac{1}{r}\frac{\partial U_r}{\partial \theta} + \frac{-U_\theta}{r} + \frac{1}{r}\frac{\partial U_\theta}{\partial r} \quad \varepsilon_{z\theta} = \frac{1}{r}\frac{\partial U_z}{\partial \theta} + \frac{\partial U_\theta}{\partial z} \quad \varepsilon_{rz} = \frac{\partial U_r}{\partial z} + \frac{\partial U_z}{\partial r}$$

We obtain the stresses in terms of strains using Hooke's law.

$$p_r = \lambda\Delta + 2\mu\varepsilon_r \quad p_\theta = \lambda\Delta + 2\mu\varepsilon_\theta \quad p_z = \lambda\Delta + 2\mu\varepsilon_z \tag{12}$$
$$p_{r\theta} = \mu\varepsilon_{r\theta} \qquad p_{rz} = \mu\varepsilon_{rz} \qquad p_{\theta z} = \mu\varepsilon_{\theta z}$$

where $\Delta$ is a dilatation defined by

$$\Delta = \varepsilon_r + \varepsilon_\theta + \varepsilon_z$$

which by substitution can be shown to equal

$$\Delta = \nabla^2 \phi$$

By proper algebraic manipulation we can obtain stress and strain in terms of displacement potentials $\phi, \psi, \chi$. In most problems, boundary conditions consisting of either the continuity or the vanishing or radial stress $p_r$ and tangential stress $p_{rz}$ arise. Therefore these two terms are written out below

$$p_r = \lambda\nabla^2\phi + 2\mu\frac{\partial}{\partial r}\left(\frac{\partial \phi}{\partial r} + \frac{\partial^2 \psi}{\partial r \partial z} + \frac{1}{r}\frac{\partial \chi}{\partial \theta}\right) \tag{13}$$
$$p_{rz} = \mu\left(\frac{\partial^2 \phi}{\partial r \partial z} + \frac{\partial^3 \psi}{\partial z^2 \partial r} + \frac{1}{r}\frac{\partial^2 \chi}{\partial z \partial \theta} + \frac{\partial^2 \phi}{\partial r \partial z} - \frac{\partial}{\partial r}\left(\frac{1}{r}\frac{\partial}{\partial r}\left(r\frac{\partial \psi}{\partial r}\right)\right) - \frac{\partial}{\partial r}\left(\frac{1}{r^2}\frac{\partial^2 \psi}{\partial \theta^2}\right)\right)$$
$$p_{rz} = \mu\left(2\frac{\partial^2 \phi}{\partial r \partial z} + \frac{1}{r}\frac{\partial^2 \chi}{\partial z \partial \theta} - \frac{\partial}{\partial r}\left(\nabla^2 \psi - 2\frac{\partial^2 \psi}{\partial z^2}\right)\right)$$

With the preceding development the equations of motion in an isotropic homogeneous medium (Aki and Richards, 1980; Harkrider, 1964)

$$(\lambda + 2\mu)\nabla(\nabla \cdot \vec{U}) + \mu\nabla \times (\nabla \times \vec{U}) = \rho\frac{\partial^2 \vec{U}}{\partial t^2} \tag{14}$$

are now satisfied implicitly by

$$\nabla^2\phi = \frac{1}{\alpha^2}\frac{\partial^2\phi}{\partial t^2} \tag{15}$$

$$\nabla^2\psi = \frac{1}{\beta^2}\frac{\partial^2\psi}{\partial t^2}$$

$$\nabla^2\chi = \frac{1}{\beta^2}\frac{\partial^2\chi}{\partial t^2}$$

where $\alpha^2 = \frac{\lambda+2\mu}{\rho}$ and $\beta^2 = \frac{\mu}{\rho}$ and $\nabla^2$ is the unadulterated Laplacian operator (Eq. 4). Lamé's theorem (Miklowitz, 1980, pg. 58–62;, Aki and Richards, 1980) allows us to define these wave equations from the initial Helmholtz vector separation. Lamé's theorem for the most general case will not be proved here because of the complexity of the algebra involved. However, an outline of the summation of radial and vertical forces leading to the algebra necessary to solve Lamé's theorem will be presented below for the axisymmetric case where $\psi$ is recoded.

### Strategy 2 - axisymmetry, recoding of the potential $\psi$ to $\psi'$

Axisymmetry, sometimes called azimuthal symmetry, implies that there is no variation allowed in properties or sources with respect to azimuth ($\theta$). This strategy is the most frequently used in the literature for modelling wave propagation inside a borehole (Biot, 1952; White, 1965) and is analogous to the case of two-dimensional propagation in Cartesian media (Ewing et al., 1957). Discontinuities are allowed in radial and axial (tangential) stresses only precluding the description of torsional sources which will be discussed later. However, axisymmetric torsional sources can be superposed with radial and axial stresses and will not affect the calculations or analysis.

$U_\theta$ and derivatives with respect to $\theta$ in the displacement potential relations (Eq. 10) vanish. With axisymmetry, $\vec{K}$ is tangent to a circle perpendicular to the $z$ axis and has no radial or vertical component $K_r, K_z = 0, \chi = 0$ such that Eq. 8 is rewritten

$$\vec{K} = -\hat{e}_\theta\frac{\partial\psi}{\partial r} \tag{16}$$

With axisymmetry the gauge condition $\nabla\cdot\vec{K} = 0$ is automatically satisfied since $\frac{\partial\chi}{\partial z} = 0$ identically. So $P$-$Sv$ and $Sh$ motion are decoupled. The quantity $-\frac{\partial\psi}{\partial r}$ is

taken as the $\theta$ component of a new displacement potential $\psi' = -\frac{\partial \psi}{\partial r}$ which maintains the symbolism of $\psi$ but this is done for good cause. Because of the widespread use of this procedure for axisymmetric media, many authors immediately use this formulation without first recognizing that $\psi$ has been recoded. The reason this recoding is used is that first it helps simplify the algebra which can be daunting at times. Secondly, this strange relationship helps maintain the analogy between axisymmetric propagation in Cartesian media $(x, y, z)$ and axisymmetric propagation governed by a cylindrical coordinate system. For instance, in Cartesian media when propagation is independent of one component, $y$ for instance, then $\vec{\psi}(\psi_x, \psi_y, \psi_z)$ has only a $\psi_y$ component. Therefore, to simplify the algebra $\frac{\partial \psi_y}{\partial x}$ is abbreviated as $\psi$, similarly for cylindrical coordinates where $\psi_\theta = -\frac{\partial \psi}{\partial r}$ is abbreviated as $\psi$ or here as $\psi'$ (Pilant, 1979, pg. 45). Ewing et al. (1957, pg. 10) equate $\psi'$ to $W$ and use $\psi$ for their derivations.

Rewriting the cross product $\nabla \times \vec{K}$ (Eq. 9) and simplifying in terms of the new potential $\psi'$, we get

$$\nabla \times \vec{K} = -\hat{e}_r\left(\frac{\partial \psi'}{\partial z}\right) + \hat{e}_z\left(\frac{1}{r}\frac{\partial}{\partial r}(r\psi')\right) \tag{17}$$

Combining $\nabla\phi$ (Eq. 2) and using the Helmholtz representation (Eq. 6) as before we get the displacement potential relations

$$U_r = \frac{\partial \phi}{\partial r} - \frac{\partial \psi'}{\partial z} \tag{18}$$

$$U_z = \frac{\partial \phi}{\partial z} + \frac{1}{r}\left(\frac{\partial}{\partial r}(r\psi')\right)$$

The same strain displacement relations (Eq. 11) apply but with terms set to zero because of the independence of $\theta$. These simplified strain displacement relations are

$$\varepsilon_r = \frac{\partial U_r}{\partial r} \quad \varepsilon_\theta = \frac{U_r}{r} \quad \varepsilon_z = \frac{\partial U_z}{\partial z} \tag{19}$$

$$\varepsilon_{r\theta} = 0 \quad \varepsilon_{z\theta} = 0 \quad \varepsilon_{rz} = \frac{\partial U_r}{\partial z} + \frac{\partial U_z}{\partial r}$$

Similarly the stresses simplify using Hooke's law.

$$p_r = \lambda\Delta + 2\mu\varepsilon_r \quad p_\theta = \lambda\Delta + 2\mu\varepsilon_\theta \quad p_z = \lambda\Delta + 2\mu\varepsilon_z \tag{20}$$

$$p_{r\theta} = 0 \qquad p_{rz} = \mu\varepsilon_{rz} \qquad p_{\theta z} = 0$$

where $\Delta$ is a dilatation defined before (Eq. ).

A brief outline of Lamé's theorem follows. First the equations of motion are developed after White, 1983. Referring to Figure 1 we determine stresses and resulting forces over a cylindrical element. The volume of the cylindrical element is $r\Delta\theta\Delta r\Delta z$. The area of the faces is approximately $r\Delta\theta\Delta r$ for the $z$ face (top), $\Delta r\Delta z$ for the $\theta$ face, $r\Delta\theta\Delta z$ and $(r+\Delta r)\Delta\theta\Delta z$ for the $r$ faces.

Referring to Figure 2 we desire to sum forces in both the radial and vertical direction. We derive the forces by summing the oppositely directed stresses multiplied by the area of application and dividing by the volume of the cylindrical element. Areas of application for each stress are indicated by a hashed pattern. Because of axisymmetry there are no net $\theta$ forces but $\theta$ components do contribute to the radial force (White, 1983). Elongation in the $r$ and $z$ direction indicated by a dashed outline contributes an extra term to the sum over $p_{zr}$ in the radial direction and $p_z$ in the vertical. The sum of these forces is equal to mass times acceleration so we obtain (White, 1983, pg. 162-164)

$$\frac{\partial p_r}{\partial r} + \frac{p_r - p_\theta}{r} + \frac{\partial p_{rz}}{\partial z} = \rho\frac{\partial^2 U_r}{\partial t^2} \tag{21}$$

$$\frac{\partial p_{rz}}{\partial r} + \frac{p_{rz}}{r} + \frac{\partial p_z}{\partial z} = \rho\frac{\partial^2 U_z}{\partial t^2} \tag{22}$$

Proceeding with Lamé's theorem we now substitute our stresses in terms of strains and strains in terms of potentials into Eq. 21 and Eq. 22. Before doing so we can examine the displacement potential relations and see that there are no interdependencies, i.e., terms in $\phi$ are independent of terms $\psi'$ so we can solve each equation in terms of $\phi$ and then $\psi'$.

Substituting the following stress potential relations into Eq. 21

$$\frac{\partial p_r}{\partial r} = (\lambda+2\mu)\frac{\partial^3\phi}{\partial r^3} + \lambda\frac{\partial}{\partial r}\left(\frac{1}{r}\frac{\partial\phi}{\partial r}\right) + \lambda\frac{\partial^3\phi}{\partial r\partial z^2} \tag{23}$$

$$\frac{p_r - p_\theta}{r} = 2\mu\frac{\partial}{\partial r}\left(\frac{1}{r}\frac{\partial\phi}{\partial r}\right)$$

$$\frac{\partial p_{rz}}{\partial z} = 2\mu\frac{\partial^3\phi}{\partial r\partial z^2}$$

and then summing

$$(\lambda+2\mu)\left(\frac{\partial^3\phi}{\partial r^3} + \frac{\partial^3\phi}{\partial r\partial z^2} + \frac{\partial}{\partial r}\left(\frac{1}{r}\frac{\partial\phi}{\partial r}\right)\right) = \rho\frac{\partial^3\phi}{\partial r\partial t^2} \tag{24}$$

Factoring out a $\frac{\partial}{\partial r}$ we obtain the wave equation independent of $\theta$.

$$\frac{\partial^2\phi}{\partial r^2} + \frac{\partial^2\phi}{\partial z^2} + \frac{1}{r}\frac{\partial\phi}{\partial r} = \frac{1}{\alpha^2}\frac{\partial^2\phi}{\partial t^2} \tag{25}$$

We can perform the same procedure for $\psi'$ yielding

$$\frac{\partial^2\psi'}{\partial r^2} + \frac{1}{r}\frac{\partial\psi'}{\partial r} - \frac{\psi'}{r^2} + \frac{\partial^2\psi'}{\partial z^2} = \frac{1}{\beta^2}\frac{\partial^2\psi'}{\partial t^2} \tag{26}$$

These new equations of motion are analogous to the wave equations in Eq. 15 and often are abbreviated $\nabla^2\phi$ and $\nabla^2\psi'$. Again the $\psi'$ has been recoded for this case so the Laplacian operation on $\psi'$ ($\nabla^2\psi'$) is adulterated. Using these equations and carrying out some algebra we can rewrite $p_r$,$p_{rz}$ as

$$p_r = \rho\frac{\partial^2\phi}{\partial t^2} - 2\mu\left(\frac{1}{r}\frac{\partial\phi}{\partial r} + \frac{\partial^2\phi}{\partial z^2} + \frac{\partial^2\psi}{\partial r\partial z}\right) \tag{27}$$

$$p_{rz} = \rho\frac{\partial^2\psi}{\partial t^2} - 2\mu\left(\frac{\partial^2\psi}{\partial z^2} - \frac{\partial^2\phi}{\partial r\partial z}\right) \tag{28}$$

A quick exercise will show that we can recover the unadulterated Laplacian operator from Eq. 26 by substituting in our original definition, *new* $\psi' = -\frac{\partial\psi'}{\partial r}$. By doing so we obtain

$$-\frac{\partial}{\partial r}\frac{\partial^2\psi'}{\partial r^2} - \frac{\partial}{\partial r}\left(\frac{1}{r}\frac{\partial\psi'}{\partial r}\right) - \frac{\partial}{\partial r}\left(\frac{\partial^2\psi'}{\partial z^2}\right) = -\frac{\partial}{\partial r}\left(\frac{1}{\beta^2}\frac{\partial^2\psi'}{\partial t^2}\right) \tag{29}$$

Dividing out the common factor of $\frac{\partial}{\partial r}$ from both sides we obtain

$$\frac{\partial^2\psi'}{\partial r^2} + \frac{1}{r}\frac{\partial\psi'}{\partial r} + \frac{\partial^2\psi'}{\partial z^2} = \frac{1}{\beta^2}\frac{\partial^2\psi'}{\partial t^2} \tag{30}$$

our original Laplacian operator as a function of our uncoded $\psi'$.

### Strategy 3 - axisymmetry, no recoding of $\psi$

This strategy is identical to strategy two except $\psi$ maintains its original definition from case 1. It's used more often in applied physics and mechanics literature than geophysics literature but this literature is often encountered. However, two very important references in the geophysics literature use this strategy, Heelan (1952, 1953) and Ewing et al. (1957). The sources must be compressional waves as is a radial source

in a borehole but mode conversion is allowed at interfaces. $U_\theta$, $\chi$, and derivatives with respect to $\theta$ are set to zero (Miklowitz, 1980). Rewriting Eq. 16

$$\begin{aligned} \vec{K} &= \hat{e}_\theta \left(-\frac{\partial \psi}{\partial r}\right) \\ \nabla \times \vec{K} &= \hat{e}_r\left(\frac{\partial^2 \psi}{\partial r \partial z}\right) - \hat{e}_z \left(\frac{1}{r}\frac{\partial}{\partial r}\left(r\frac{\partial \psi}{\partial r}\right)\right). \end{aligned} \tag{31}$$

As with the previous axisymmetric treatment, the gauge condition $\nabla \cdot \vec{K} = 0$ is now automatically satisfied since $\frac{\partial \chi}{\partial z} = 0$ identically for axisymmetry.

Summing $\nabla \times \vec{K}$ and adding it to $\nabla\phi$ using the Helmholtz representation as before we get the displacement potential relations

$$\begin{aligned} U_r &= \frac{\partial \phi}{\partial r} + \frac{\partial^2 \psi}{\partial r \partial z} \\ U_z &= \frac{\partial \phi}{\partial z} - \frac{1}{r}\frac{\partial}{\partial r}\left(r\frac{\partial \psi}{\partial r}\right). \end{aligned} \tag{32}$$

The strain-displacement relations are equivalent to those for strategy 2 (Eq. 19) but now the displacement elements $U_r, U_z$ are different. This will affect the boundary conditions, the wave equations and the form of the governing Bessel function.

$$\begin{aligned} &\varepsilon_r = \frac{\partial U_r}{\partial r} \quad \varepsilon_\theta = \frac{U_r}{r} \quad \varepsilon_z = \frac{\partial U_z}{\partial z} \\ &\varepsilon_{r\theta} = 0 \quad \varepsilon_{z\theta} = 0 \quad \varepsilon_{rz} = \frac{\partial U_r}{\partial z} + \frac{\partial U_z}{\partial r} \end{aligned} \tag{33}$$

The Hooke's law relationships (Eq. 20) remain unchanged from strategy 2 and thus are not repeated here. Because $\psi$ has not been recoded here, the simplified wave equation relationships have been maintained for $\phi, \psi$ (Eq. 15) with the Laplacian operator.

$$\begin{aligned} \frac{1}{r}\frac{\partial}{\partial r}\left(r\frac{\partial \phi}{\partial r}\right) + \frac{\partial^2 \phi}{\partial z^2} &= \frac{1}{\alpha^2}\frac{\partial^2 \phi}{\partial t^2} \\ \frac{1}{r}\frac{\partial}{\partial r}\left(r\frac{\partial \psi}{\partial r}\right) + \frac{\partial^2 \psi}{\partial z^2} &= \frac{1}{\beta^2}\frac{\partial^2 \psi}{\partial t^2} \end{aligned} \tag{34}$$

### Strategy 4 - axisymmetry, torsional motion

Torsional waves in a rod are the analog of $Sh$ waves in a plate. A second type of symmetry is to assume axial symmetry but to require purely torsional sources (Miklowitz, 1978, pg. 217–220; White, 1983). Because of the axisymmetry, derivatives with respect to $\theta$ vanish and $U_r, U_z$ are zero. Since $U_r, U_z$ are equal to zero $\phi, \psi = 0$

$\vec{K}$ can be rewritten

$$\begin{aligned} \vec{K} &= \hat{e}_z(\chi) \\ \nabla \times \vec{K} &= -\hat{e}_\theta \frac{\partial \chi}{\partial r}. \end{aligned} \tag{35}$$

The gauge condition $\nabla \cdot \vec{K} = 0$ is not necessarily satisfied here since $\nabla \cdot \vec{K} = \frac{\partial \chi}{\partial z}$. But $Sh$ motion is decoupled because $\phi, \psi$ equal zero identically. By utilizing the Helmholtz representation again we obtain

$$U_\theta = -\frac{\partial \chi}{\partial r}. \tag{36}$$

Simplifying the strain displacement relationships and Hooke's law

$$\begin{aligned} \varepsilon_{r\theta} = r\frac{\partial}{\partial r}(\frac{U_\theta}{r}) \quad \varepsilon_{\theta z} = \frac{\partial U_\theta}{\partial z} \\ p_{r\theta} = \mu \varepsilon_{r\theta} \quad p_{\theta z} = \mu \varepsilon_{\theta z} \end{aligned} \tag{37}$$

the remaining stress and strain elements equalling zero.

$\chi$ satisfies the wave equation (Eq. 15)

$$\frac{\partial^2 \chi}{\partial r^2} + \frac{1}{r}\frac{\partial \chi}{\partial r} + \frac{\partial^2 \chi}{\partial z^2} = \frac{1}{\beta^2}\frac{\partial^2 \chi}{\partial t^2}. \tag{38}$$

### Strategy 5 - nonaxisymmetric, propagation independent of z

This strategy has been adopted by Sezawa (1927), Viktorov (1958), Siggins and Stokes (1987), and Siggins (1989) to calculate wave propagation emanating from line sources. Because of the symmetry in $z$, derivatives with respect to $z$ must vanish. This implies $\psi$ equal to zero by taking $\nabla \times \vec{K}$. Unfortunately, Viktorov, Siggins and Stokes, and Siggins chose to use the potential $\psi$ for $\chi$.

$\vec{K}$ is rewritten

$$\begin{aligned} \vec{K} &= \hat{e}_z(\chi) \\ \nabla \times \vec{K} &= \hat{e}_r(\frac{1}{r}\frac{\partial \chi}{\partial \theta}) - \hat{e}_\theta(\frac{\partial \chi}{\partial r}). \end{aligned} \tag{39}$$

Like case 4 and case 1, the gauge condition is not necessarily satisfied here since $\nabla \cdot \vec{K} = \frac{\partial \psi}{\partial z}$. Therefore $P$ and $Sh$ motions are coupled through the boundary conditions. The displacement potential relations using the Helmholtz representation (Eq. 6) are

$$\begin{aligned} U_r &= \frac{\partial \phi}{\partial r} + \frac{1}{r}\frac{\partial \chi}{\partial \theta} \\ U_\theta &= \frac{1}{r}\frac{\partial \phi}{\partial \theta} - \frac{\partial \chi}{\partial r}. \end{aligned} \tag{40}$$

Applying the strain-displacement relations (Eq. 11) we obtain

$$\begin{aligned} \varepsilon_r &= \frac{\partial U_r}{\partial r} \\ \varepsilon_\theta &= \frac{1}{r}\left(\frac{\partial U_\theta}{\partial \theta} + U_r\right) \\ \varepsilon_{r\theta} &= \frac{1}{r}\frac{\partial U_r}{\partial \theta} + r\frac{\partial}{\partial r}\left(\frac{U_\theta}{r}\right). \end{aligned} \tag{41}$$

Again, we can use Hooke's law to obtain stresses in terms of strains and $\phi, \chi$ satisfy the wave equations (Eq. 15) with dependence on $z$ removed.

$$\begin{aligned} \frac{1}{r}\frac{\partial}{\partial r}\left(r\frac{\partial \phi}{\partial r}\right) + \frac{1}{r^2}\frac{\partial^2 \phi}{\partial \theta^2} &= \frac{1}{\alpha^2}\frac{\partial^2 \phi}{\partial t^2} \\ \frac{1}{r}\frac{\partial}{\partial r}\left(r\frac{\partial \chi}{\partial r}\right) + \frac{1}{r^2}\frac{\partial^2 \chi}{\partial \theta^2} &= \frac{1}{\beta^2}\frac{\partial^2 \chi}{\partial t^2} \end{aligned} \tag{42}$$

## Transforming the resultant wave equations using separation of variables

When no symmetry assumptions were made we obtained wave equations of the form

$$\begin{aligned} \frac{\partial^2 \phi}{\partial r^2} + \frac{1}{r}\frac{\partial \phi}{\partial r} + \frac{1}{r^2}\frac{\partial^2 \phi}{\partial \theta^2} + \frac{\partial^2 \phi}{\partial z^2} &= \frac{1}{\alpha^2}\frac{\partial^2 \phi}{\partial t^2} \\ \frac{\partial^2 \psi}{\partial r^2} + \frac{1}{r}\frac{\partial \psi}{\partial r} + \frac{1}{r^2}\frac{\partial^2 \psi}{\partial \theta^2} + \frac{\partial^2 \psi}{\partial z^2} &= \frac{1}{\beta^2}\frac{\partial^2 \psi}{\partial t^2} \\ \frac{\partial^2 \chi}{\partial r^2} + \frac{1}{r}\frac{\partial \chi}{\partial r} + \frac{1}{r^2}\frac{\partial^2 \chi}{\partial \theta^2} + \frac{\partial^2 \chi}{\partial z^2} &= \frac{1}{\beta^2}\frac{\partial^2 \chi}{\partial t^2} \end{aligned} \tag{43}$$

where the left hand side is the unadulterated Laplacian (Eq. 4) of each potential.

Proposed solutions are of the form

$$\phi(r,\theta,z,t) = R(r)\Theta(\theta)Z(z)T(t) \tag{44}$$

and similarly for $\psi, \chi$.

The general procedure for separation of variables is presented in texts on differential equations. The exercise will be performed here for the potential $\phi$, the procedure for $\psi, \chi$ being identical. Our goal will be to obtain equations in terms of exponential and Bessel functions. Substituting this proposed form for $\phi$ (Eq. 44) into Eq. 43 and dividing by $\phi$ we get five quotients in our equation. Each quotient contains only one dependent variable. The quotient $\frac{R''}{R}$ for instance is dependent on $r$ and not on $z, \theta, t$ etc. For brevity's sake the functional dependencies have been omitted.

$$\alpha^2 \left[ \frac{R''}{R} + \frac{1}{r}\frac{R'}{R} + \frac{1}{r^2}\frac{\Theta''}{\Theta} + \frac{Z''}{Z} \right] = \frac{T''}{T} \tag{45}$$

Setting the right hand side of this equation equal to the parameter $-\omega^2$ we get an ordinary differential equation with exponential solution.

$$\begin{aligned} \frac{T''}{T} &= -\omega^2 \\ T(t) &= e^{i\omega t} \end{aligned} \tag{46}$$

$\omega$ is the radial frequency term and the positive sign of $\omega$ is crucial to the subsequent development. The $e^{i\omega t}$ is commonly referred to as the time dependence. The most common convention in geophysics is to use the time dependence $e^{i\omega t}$ (White, 1965; White and Zechman, 1968; Greenfield, 1978; Schoenberg et al., 1981; Balch and Lee, 1984; Lee 1986). An $e^{-i\omega t}$ time dependence is found in some geophysical literature (Heelan, 1953; Tsang and Rader, 1979; Tsang and Kong, 1979; Aki and Richards, 1980; Cheng and Toksöz, 1981; Cheng et al., 1982).

We will soon calculate wavenumbers which are square root functions, the difference in phase of the square root will be a factor of $i$ if the time dependence is negative instead of positive. This difference in phase allows authors to substitute modified Bessel functions for Bessel functions and vice versa since the modified Bessel functions are fundamentally Bessel functions of imaginary argument.

Rewriting Eq. 45 after some rearrangement we get

$$\frac{R''}{R} + \frac{1}{r}\frac{R'}{R} + \frac{1}{r^2}\frac{\Theta''}{\Theta} + \frac{\omega^2}{\alpha^2} = -\frac{Z''}{Z}. \tag{47}$$

Again setting the right hand side equal to a parameter, this time $k_z^2$ we obtain

$$\begin{aligned} \frac{Z''}{Z} &= -k_z^2 \\ Z(z) &= -e^{-ik_z z}. \end{aligned} \tag{48}$$

The most common convention regarding $k_z$, the axial wavenumber, is to use the opposite sign to that of radial frequency $\omega$.

Rearranging Eq. 47 and multiplying both sides by $r^2$

$$r^2\left[\frac{R''}{R} + \frac{1}{r}\frac{R'}{R} - k_z^2 + \frac{\omega^2}{\alpha^2}\right] = -\frac{\Theta''}{\Theta}. \tag{49}$$

The left hand side is again independent of $\theta$ so we set the right hand side to equal the parameter $n^2$.

$$\begin{aligned} \frac{\Theta''}{\Theta} &= -n^2 \\ \Theta(\theta) &= -e^{in\theta} \end{aligned} \tag{50}$$

The sign of $n$ is almost always positive by convention. By Euler's formula we can decompose the term $e^{in\theta}$ into a sum of sines and cosines. For the most general solution of the potential we will be summing up an infinite number of these terms. For the terms to remain single valued in the variable $\theta$ they must replicate with a period of $2\pi$. For this to happen, $n$ must be an integer (Lee, 1986).

Dividing both sides by $r^2$ and multiplying through by $R$

$$R'' + \frac{1}{r}R' + \left(-k_z^2 + \frac{\omega^2}{\alpha^2} - \frac{n^2}{r^2}\right)R = 0. \tag{51}$$

This is a Bessel's equation of order $n$ (Bowman, 1958). Solutions are Bessel functions of the first, $J_{\pm n}(lr)$, second, $Y_n(lr)$ and third kind, $H_n^{(1)}(lr), H_n^{(2)}(lr)$ (Abramowitz and Stegun, 1964,Eq. 9.1.1). Bessel functions of the third kind are known as Hankel functions. $n$ is the order of the Bessel function. $l$ is a radial wavenumber $l = \sqrt{\frac{\omega^2}{\alpha^2} - k_z^2}$.

The modified Bessel functions $I_n(z), K_n(z)$ are fundamentally Bessel functions of imaginary argument times a constant. Therefore $I_n(ilr), K_n(ilr)$ are also solutions. By putting $l' = il$ where $l' = \sqrt{k_z^2 - \frac{\omega^2}{\alpha^2}}$ we have $I_n(l'r)$ and $K_n(l'r)$ as solutions. For the potentials $\psi, \chi$ solutions are of the same general form but with a new radial wavenumber $m$ which equals $\sqrt{\frac{\omega^2}{\beta^2} - k_z^2}$.

Although the Bessel functions and modified Bessel functions each solve Bessel's equation of order n, only in combinations do they span the whole space of possible

solutions. General solutions for each $R_n$ are any of the following.

$$R_n = A_{nJY}J_n(lr) + B_{nJY}Y_n(lr) \quad (52)$$
$$R_n = A_{nH}H_n^{(1)}(lr) + B_{nH}H_n^{(2)}(lr) \quad (53)$$
$$R_n = A_{nKI}K_n(l'r) + B_{nKI}I_n(l'r) \quad (54)$$

where $A_n, B_n$ are coefficients and functions of $k_z, \omega, \theta$. The superscript on $n$ designates the type of Bessel function the general solution is constructed of. The first two general solutions (Eq. 52,Eq. 53) can easily be seen to be equivalent. Recalling a basic property of Bessel functions (Abramowitz and Stegun, 1964)

$$H_n^{(1)}(z) = J_n(z) + iY_n(z) \quad (55)$$
$$H_n^{(2)}(z) = J_n(z) - iY_n(z)$$

we can solve a simple $2 \times 2$ set of equations to yield $A_{nH}, B_{nH}$ in terms of $A_{nJY}, B_{nJY}$.

We allow all solutions of $\phi$ to be superposed. Therefore we integrate over all $k_z$, all of $\omega$, and integer values of $n$. Hence solutions for $\phi$ are any of the following

$$\phi = \sum_{n=-\infty}^{\infty} \int\int_{-\infty}^{\infty} (A_{nJY}J_n(lr) + B_{nJY}Y_n(lr))e^{-ik_z z}e^{i\omega t}e^{in\theta}dk_z\, d\omega \quad (56)$$
$$\phi = \sum_{n=-\infty}^{\infty} \int\int_{-\infty}^{\infty} (A_{nH}H_n^{(1)}(lr) + B_{nH}H_n^{(2)}(lr))e^{-ik_z z}e^{i\omega t}e^{in\theta}dk_z\, d\omega$$
$$\phi = \sum_{n=-\infty}^{\infty} \int\int_{-\infty}^{\infty} (A_{nKI}K_n(l'r) + B_{nKI}I_n(l'r))e^{-ik_z z}e^{i\omega t}e^{in\theta}dk_z\, d\omega$$

using the outlined sign conventions above. $\psi, \chi$ are similarly represented but with wavenumbers $m, m'$ instead of $l, l'$.

$$\psi = \sum_{n=-\infty}^{\infty} \int\int_{-\infty}^{\infty} (C_{nKI}K_n(m'r) + D_{nKI}I_n(m'r))e^{-ik_z z}e^{i\omega t}e^{in\theta}dk_z\, d\omega \quad (57)$$
$$\chi = \sum_{n=-\infty}^{\infty} \int\int_{-\infty}^{\infty} (E_{nKI}K_n(m'r) + F_{nKI}I_n(m'r))e^{-ik_z z}e^{i\omega t}e^{in\theta}dk_z\, d\omega$$

where for the sake of brevity only those solutions in terms of the modified Bessel functions are reproduced for $\psi$ and $\chi$. This pattern of designating coefficients $A, B$ for the irrotational potential $\phi$, $C, D$ for the solenoidal potential $\psi$, $E, F$ for the solenoidal potential $\chi$ will be strictly adhered to throughout.

## Use of Sommerfeld radiation conditions to reduce the dimensionality of the general integrals

The Sommerfeld radiation condition states that solutions are not allowed to increase to infinity. This means that the governing asymptotic behavior which is exponential

can not be real and positive for outgoing waves. The asymptotic behavior of solutions of Bessel's equations of order $n$ as $z$ goes to $\infty$ is the following to the first term with some subsequent simplification (Abramowitz and Stegun, 1964).

$$J_n(z) \sim \sqrt{\frac{2}{\pi z}}\cos(z - \frac{n\pi}{2} - \frac{\pi}{4}) \tag{58}$$

$$J_n(z) \sim \sqrt{\frac{1}{z}}(e^{iz} + e^{-iz}) \tag{59}$$

$$Y_n(z) \sim \sqrt{\frac{2}{\pi z}}\sin(z - \frac{n\pi}{2} - \frac{\pi}{4}) \tag{60}$$

$$Y_n(z) \sim i\sqrt{\frac{1}{z}}(e^{iz} - e^{-iz}) \tag{61}$$

$$H_n^{(1)}(z) \sim \frac{\pi}{\sqrt{2z}}e^{iz} \tag{62}$$

$$H_n^{(2)}(z) \sim \frac{\pi}{\sqrt{2z}}e^{-iz} \tag{63}$$

$$I_n(z) \sim \frac{1}{\sqrt{2\pi z}}e^{z} \tag{64}$$

$$K_n(z) \sim \sqrt{\frac{\pi}{2z}}e^{-z} \tag{65}$$

The asymptotic behavior is governed by the real part of the exponential function, the imaginary part only contributing to oscillation. The asymptotic behavior of $J_n$ (Eq. 58) and $Y_n$ (Eq. 60) is very similar and by referring to Figure 3 it can be seen that they sinusoidally decay exponentially to infinity. Additionally, $J_n$ is finite at 0 and $Y_n$ goes to $-\infty$ as $z$ goes to zero. Both $J_n, Y_n$ explode if the imaginary part of z goes to $\infty$. Our argument is $lr$ with $r$ being real and $l = \sqrt{\frac{\omega^2}{\alpha^2} - k_z^2}$. Our argument will go to imaginary infinity when $k_z^2 > \frac{\omega^2}{\alpha^2}$. What would be preferred physically is to have a pair of wave functions that have opposite asymptotic behavior so we can assign one wave function to the outgoing wave and one to the incoming. We have just shown that $J_n, Y_n$ do not satisfy this criteria, but the Hankel functions and modified Bessel functions do however. For this reason, they are found much more frequently as general solutions in wave propagation literature.

The advantage of the incoming/outgoing wave duality is that we usually limit ourselves to the calculation of outgoing waves in an infinite medium and limit ourselves to incoming waves incident on a cylindrical borehole or propagating through a borehole. This reduces computational complexity by half.

The asymptotic behavior of $K_n, I_n$ is seen for real argument in Figure 4. $K_n$ represents an outgoing wave because it decays to zero at infinity whereas $I_n$ represents an incoming wave. It's difficult to plot Hankel functions $H_n^{(1)}, H_n^{(2)}$ as was done with $J_n, Y_n$ and $K_n, I_n$ but we can discuss the behavior by substituting an $iz$ for $z$ in the

asymptotic relations. In so doing we see that $H_n^{(2)}$ resembles $K_n$ and is therefore an outgoing wave. $H_n^{(1)}$ resembles the behavior of $I_n$ and is consequently an incoming wave.

The relations just developed are valid off the axis where $r > 0$. This condition is met for media surrounding a cylinder which is the usual case treated. Inside the cylinder we have to avoid the singularities in the Bessel and modified Bessel functions at $r = 0$. For instance when Hankel functions $H_n^{(1)}, H_n^{(2)}$ are used for the general solution, there is a potential singularity at zero since $Y_n(0)$, a component of both Hankel functions (Eq. 55), approaches negative infinity as $r$ approaches 0. Therefore we set the coefficient on the Hankel functions equivalent yielding the Bessel function $J_n$ (Tsang and Rader, 1979; Cheng and Toksöz, 1981) as follows

$$AJ_n(z) = A\frac{H_n^{(1)}(z) + H_n^{(2)}(z)}{2}. \tag{66}$$

Besides the radiation conditions, another simplification is commonly introduced to the wave propagation problem with no symmetry assumptions. Flexural wave motion is governed by first order $\theta$ dependence only so the infinite summation of double integrals (Eq. 56) is reduced to a summation over $n = 1$ (Miklowitz, 1978, White, 1983).

### Separation of variables — axisymmetric media, $\psi$

For the axisymmetric case with recodified $\psi$, case 2, simplifications occur because the dependence on $\theta$ is removed and therefore the infinite sum of Bessel functions over $n$ is removed in the integrals of Eq. 56. Complications arise because we've introduced a new form of wave equation in terms of $\psi$. These wave equations are

$$\frac{\partial^2\phi}{\partial r^2} + \frac{\partial^2\phi}{\partial z^2} + \frac{1}{r}\frac{\partial\phi}{\partial r} = \frac{1}{\alpha^2}\frac{\partial^2\phi}{\partial t^2} \tag{67}$$

$$\frac{\partial^2\psi}{\partial r^2} + \frac{1}{r}\frac{\partial\psi}{\partial r} - \frac{\psi}{r^2} + \frac{\partial^2\psi}{\partial z^2} = \frac{1}{\beta^2}\frac{\partial^2\psi}{\partial t^2}.$$

Proposed solutions are of the form

$$\phi(r,z,t) = R_\phi(r)Z(z)T(t) \tag{68}$$

$$\psi(r,z,t) = R_\psi(r)Z(z)T(t). \tag{69}$$

The two solutions for $R_\phi, R_\psi$ will not be equivalent. Following the sign conventions for the first case with no symmetry assumptions made we obtain two equations for $R$ to be solved. For $\phi$

$$R''_\phi(r) + \frac{1}{r}R'_\phi(r) + \left(-k_z^2 + \frac{\omega^2}{\alpha^2}\right) R = 0. \tag{70}$$

and for $\psi$

$$R''_\psi(r) + \frac{1}{r}R'_\psi(r) + \left(-k_z^2 + \frac{\omega^2}{\beta^2} - \frac{1}{r^2}\right) R = 0 \tag{71}$$

The equation for $R_\phi$ is seen to be a Bessel's equation of order 0 and similarly the solution for $R_\psi$ a Bessel's equation of order one. Solutions for $R_\phi, R_\psi$ can be represented in the following forms using Bessel, modified Bessel and Hankel functions

$$\begin{aligned} R_\phi(r) &= A_{JY}J_0(lr) + B_{JY}Y_0(lr) \qquad (72)\\ R_\phi(r) &= A_H H_0^{(1)}(lr) + B_H H_0^{(2)}(lr) \\ R_\phi(r) &= A_{KI}K_0(l'r) + B_{KI}I_0(l'r) \\ R_\psi(r) &= C_{JY}J_0(lr) + D_{JY}Y_0(lr) \qquad (73)\\ R_\psi(r) &= C_H H_1^{(1)}(mr) + D_H H_1^{(2)}(mr) \\ R_\psi(r) &= C_{KI}K_1(m'r) + D_{KI}I_1(m'r). \end{aligned}$$

(74)

Again following the argument regarding the Sommerfeld radiation condition of the preceding section, it is easy to recognize $K_0, K_1, H_0^{(2)}, H_1^{(2)}$ as outgoing waves and $I_0, I_1, H_0^{(1)}(), H_1^{(1)}$ as incoming waves. The use of the modified Bessel functions $K$ and $I$ is made by Biot (1952), White (1983), Cheng et al. (1982) and many others and is the most common for describing wave propagation inside an axisymmetric borehole. The use of Hankel functions is made by White (1965). Both systems are used by Cheng and Toksöz (1981). Tsang and Rader (1979) use both Hankel functions and Bessel functions.

Writing the resulting integrals which are recognized as a double Fourier transform in $k_z$ and $\omega$ we obtain the following.

$$\begin{aligned} \phi &= \int\!\!\int_{-\infty}^{\infty} (A_{KI}K_0(l'r) + B_{KI}I_0(l'r))e^{-ik_z z}e^{i\omega t}dk_z\, d\omega \qquad (75)\\ \phi &= \int\!\!\int_{-\infty}^{\infty} (A_H H_0^{(1)}(lr) + B_H H_1^{(1)}(lr))e^{-ik_z z}e^{i\omega t}dk_z\, d\omega \end{aligned}$$

$$\psi = \int\int_{-\infty}^{\infty} (C_{KI} K_1(l'r) + D_{KI} I_1(l'r)) e^{-ik_z z} e^{i\omega t} dk_z \, d\omega$$
$$\psi = \int\int_{-\infty}^{\infty} (C_H H_0^{(2)}(lr) + D_H H_0^{(2)}(lr)) e^{-ik_z z} e^{i\omega t} dk_z \, d\omega.$$

## Separation of variables, axisymmetric media, no recoding of $\psi$

Because of the axisymmetry, dependence on $\theta$ is removed and $\chi = 0$. Exponentials in $k_z, \omega$ and definitions of radial wavenumbers $l, l', m, m'$ remain equivalent to the first case and maintain the sign conventions. We have the wave equations

$$\frac{\partial^2 \phi}{\partial r^2} + \frac{1}{r}\frac{\partial \phi}{\partial r} + \frac{\partial^2 \phi}{\partial z^2} = \frac{1}{\alpha^2}\frac{\partial^2 \phi}{\partial t^2} \tag{76}$$

$$\frac{\partial^2 \psi}{\partial r^2} + \frac{1}{r}\frac{\partial \psi}{\partial r} + \frac{\partial^2 \psi}{\partial z^2} = \frac{1}{\beta^2}\frac{\partial^2 \psi}{\partial t^2}.$$

We desire solutions of the form

$$\{\phi, \psi\} = R_{\phi,\psi}(r) Z(z) T(t). \tag{77}$$

Removing the dependence on $\theta$ we simplify the Bessel's equation of order $n$ (Eq. 51) to a Bessel's equation of order zero.

$$R''_{\phi,\psi} + \frac{1}{r} R'_{\phi,\psi} + \left( -k_z^2 + \frac{\omega^2}{\{\alpha, \beta\}^2} \right) R_{\phi,\psi} = 0. \tag{78}$$

Rewriting the integrals (Eq. 56) and restricting ourselves to modified Bessel and Hankel functions as before we obtain

$$\phi = \int\int_{-\infty}^{\infty} (A_{KI} K_0(l'r) + B_{KI} I_0(l'r)) e^{-ik_z z} e^{i\omega t} dk_z \, d\omega \tag{79}$$
$$\phi = \int\int_{-\infty}^{\infty} (A_H H_0^{(1)}(lr) + B_H H_1^{(1)}(lr)) e^{-ik_z z} e^{i\omega t} dk_z \, d\omega$$
$$\psi = \int\int_{-\infty}^{\infty} (C_{KI} K_0(m'r) + D_{KI} I_0(m'r)) e^{-ik_z z} e^{i\omega t} dk_z \, d\omega$$
$$\psi = \int\int_{-\infty}^{\infty} (C_H H_0^{(1)}(mr) + D_H H_0^{(2)}(mr)) e^{-ik_z z} e^{i\omega t} dk_z \, d\omega$$

which are again recognized as double Fourier transforms and the superposition of incoming and outgoing waves.

### Separation of variables, axisymmetry, torsional sources

We have wave equations of the form

$$\frac{\partial^2 \chi}{\partial r^2} + \frac{1}{r}\frac{\partial \chi}{\partial r} + \frac{\partial^2 \chi}{\partial z^2} = \frac{1}{\beta^2}\frac{\partial^2 \chi}{\partial t^2} \tag{80}$$

and desire solutions of the form

$$\chi = R_\chi(r)Z(z)T(t) \tag{81}$$

where $R_\chi$ solves the following Bessel's equation of order zero

$$R_\chi'' + \frac{1}{r}R_\chi' + \left(-k_z^2 + \frac{\omega^2}{\beta^2}\right) R_\chi = 0. \tag{82}$$

Rewriting the integrals (Eq. 56) as superpositions of incoming and outgoing waves we obtain

$$\begin{aligned} \chi &= \int\int_{-\infty}^{\infty} (E_{KI}K_0(m'r) + F_{KI}I_0(m'r))e^{-ik_z z}e^{i\omega t}dk_z\, d\omega \\ \chi &= \int\int_{-\infty}^{\infty} (E_H H_0^{(1)}(mr) + F_H H_0^{(2)}(mr))e^{-ik_z z}e^{i\omega t}dk_z\, d\omega. \end{aligned} \tag{83}$$

### Separation of variables, symmetry in z

For the case of symmetry along the $z$ axis as presented in Viktorov (1958), Siggins and Stokes (1987),and Siggins (1989), we have wave equations of the form

$$\frac{\partial^2 \phi}{\partial r^2} + \frac{1}{r}\frac{\partial \phi}{\partial r} + \frac{1}{r^2}\frac{\partial^2 \phi}{\partial \theta^2} = \frac{1}{\alpha^2}\frac{\partial^2 \phi}{\partial t^2} \tag{84}$$

$$\frac{\partial^2 \chi}{\partial r^2} + \frac{1}{r}\frac{\partial \phi}{\partial r} + \frac{1}{r^2}\frac{\partial^2 \chi}{\partial \theta^2} = \frac{1}{\beta^2}\frac{\partial^2 \phi}{\partial t^2}$$

we desire solutions of the form

$$\{\phi, \chi\} = R_{\phi,\chi}(r)Z(z)T(t) \tag{85}$$

where $R_{\phi,\chi}$ solves the following Bessel's equation of order n.

$$R_{\phi,\chi}'' + \frac{1}{r}R_{\phi,\chi}' + \left(-k_z^2 + \frac{\omega^2}{\{\alpha,\beta\}^2} - \frac{n^2}{r^2}\right) R_{\phi,\chi} = 0 \tag{86}$$

Rewriting the integrals (Eq. 56) as superpositions of incoming and outgoing waves and utilizing the previously defined sign and wavenumber conventions

$$\phi = \sum_{n=-\infty}^{\infty}\int_{-\infty}^{\infty}(A_{KI}K_n(l'r) + B_{KI}I_n(l'r))e^{i\omega t}e^{in\theta}\,d\omega$$

$$\phi = \sum_{n=-\infty}^{\infty}\int_{-\infty}^{\infty}(A_H H_n^{(1)}(lr) + B_H H_n^{(2)}(lr))e^{i\omega t}e^{in\theta}\,d\omega$$

$$\chi = \sum_{n=-\infty}^{\infty}\int_{-\infty}^{\infty}(E_{KI}K_n(m'r) + F_{KI}I_n(m'r))e^{i\omega t}e^{in\theta}\,d\omega$$

$$\chi = \sum_{n=-\infty}^{\infty}\int_{-\infty}^{\infty}(E_H H_n^{(1)}(mr) + F_H H_n^{(2)}(mr))e^{i\omega t}e^{in\theta}e^{in\theta}\,d\omega.$$

In formulating our propagation independent of $z$, we have thus eliminated one of the integrals over minus infinity to plus infinity.

## SOURCE RADIATION PATTERNS FROM DOWNHOLE SOURCES, POINT SOURCES

This section will show the development of the impulse response for a point source centered in a fluid-filled borehole surrounded by an infinite, elastic, isotropic, axisymmetric medium. Synthetic seismograms will qualitatively and quantitatively show near field effects.

### Homogeneous Problem - General Solution

Assume an infinite isotropic axisymmetric fluid or solid medium to be described in cylindrical coordinates. The displacement field can be represented by three displacement potentials $\phi, \psi, \chi$ corresponding to a longitudinal $\phi$ and transverse $\psi, \chi$ waves. Each displacement potential implicitly solves a wave equation (Eq. 25, Eq. 26) by Lamé's theorem. Assuming axisymmetry, $P - Sv$ and $Sh$ motions are uncoupled and only $P - Sv$ motion will be considered here. As in Cartesian media, $\psi$ can be recoded to $\psi'$ so that the displacement-potential relations, the proof of Lamé's theorem and algebra in general are simpler (Pilant, 1979). The recoding is $\psi' = -\dfrac{\partial \psi}{\partial r}$. To facilitate comparison with previous work in axisymmetric media, the recoded $\psi'$ will be used in the following development.

By recoding $\psi$ to $\psi'$ the wave equation and displacement potential relations are of a different form for $\psi'$ but remain equivalent for the unchanged $\psi$. The interrelationship

between this axisymmetric treatment and the four other symmetry systems commonly considered in wave propagation problems in cylindrical coordinates is discussed extensively in the previous section. The wave equations (Eq. 25, Eq. 26) are

$$\begin{aligned} \nabla^2\phi = & \quad \frac{\partial^2\phi}{\partial r^2} + \frac{1}{r}\frac{\partial\phi}{\partial r} + \frac{\partial^2\phi}{\partial z^2} \quad = \frac{1}{\alpha^2}\frac{\partial^2\phi}{\partial t^2} \\ \nabla^2\psi' = & \quad \frac{\partial^2\psi'}{\partial r^2} + \frac{1}{r}\frac{\partial\psi'}{\partial r} - \frac{\psi'}{r^2} + \frac{\partial^2\psi'}{\partial z^2} \quad = \frac{1}{\beta^2}\frac{\partial^2\psi'}{\partial t^2}. \end{aligned} \tag{87}$$

These wave equations are separable and there are many different means of writing the general solution. The particular method here will be that adapted by White (1983) with the modified Bessel functions $K_{\{0,1\}}$ representing outgoing waves and the modified Bessel functions $I_{\{0,1\}}$ representing incoming waves. The time dependence $e^{i\omega t}$ will be positive and the sign of the axial wavenumber $k_z$ will be negative. The solutions are (Eq. 75).

$$\begin{aligned} \phi_f &= \int\int_{-\infty}^{\infty} (A_f K_0(f'r) + B_f I_0(f'r)) e^{-ik_z z} e^{i\omega t} dk_z \, d\omega \\ \psi_f &= 0 \\ \phi &= \int\int_{-\infty}^{\infty} (A K_0(l'r) + B I_0(l'r)) e^{-ik_z z} e^{i\omega t} dk_z \, d\omega \\ \psi &= \int\int_{-\infty}^{\infty} (C K_1(m'r) + D I_1(m'r)) e^{-ik_z z} e^{i\omega t} dk_z \, d\omega \end{aligned} \tag{88}$$

where $f' = \sqrt{k_z^2 - \frac{\omega^2}{\alpha_f^2}}$ and $l' = \sqrt{k_z^2 - \frac{\omega^2}{\alpha^2}}$ are compressional radial wave numbers for the fluid and solid respectively. No shear potential is supported in the fluid so $\psi_f = 0$ and the shear radial wavenumber $m' = \sqrt{k_z^2 - \frac{\omega^2}{\beta^2}}$. The constants $A_f, B_f, A, B, C, D$ are functions of $k_z$ and $\omega$ and the integrals are recognized as double Fourier transforms over $k_z$ and $\omega$. For notational convenience the integral signs and $dk_z, d\omega$ will be dropped subsequently.

In the fluid we will calculate the solution for incoming waves reflected off the borehole boundary. $r = 0$ is a pole of the function $K_0(f'r)$, see Figure 4. Therefore, $A_f$ is set to zero. In the elastic medium surrounding the fluid-filled borehole we will only calculate the solution for outgoing waves so the potentials simplify to

$$\begin{aligned} \phi_f &= B_f I_0(f'r) e^{-ik_z z} e^{i\omega t} \\ \phi &= A K_0(l'r) e^{-ik_z z} e^{i\omega t} \\ \psi &= C K_1(m'r) e^{-ik_z z} e^{i\omega t}. \end{aligned} \tag{89}$$

It's important to compare this general solution to developments in the literature. Authors who use this representation of the general solution in terms of modified Bessel

functions for axisymmetric media include Biot (1952), Cheng and Toksöz (1981, excluding appendix), Cheng et al. (1982), and White (1983). However, other authors (White, 1962,1965) use Hankel functions instead of modified Bessel functions as shown in the previous section. The substitution is $H_{0,1}^{(1)}(fr)$ for $I_{0,1}(f'r)$ and $H_{0,1}^{(2)}(fr)$ for $K_{0,1}(f'r)$ where $f = if'$ and similarly for $l, l', m, m'$. For comparison to works that use the time dependence $e^{-i\omega t}$ (Tsang and Rader, 1979; Cheng and Toksöz, 1981 Appendix), replace $J_0(fr)$ for $I_0(f'r)$ and $H_{0,1}^{(1)}(fr)$ for $K_{0,1}(f'r)$. Tsang and Rader (1979) also use Hankel functions instead of $J_0(fr)$ in the second half of their paper which deals with branch cut integration after Roever et al. (1974).

Biot (1952) uses $\phi_o, \psi_o$ for $A, C$ and formulates $B_f$ in terms of $A, C$. White (1965, 1983) uses $A_1', A_2, B_2$ for $B_f, A, C$. Tsang and Rader (1979) and Schoenberg et al. (1981) use $A, C, D$ for $B_f, A, C$. Peterson (1974) normalizes $r, z$ and the wavenumber $k_z$ by dividing through by radius $a$ and renames them $\eta, \nu, s$. Hence Peterson's results are not easily comparable with these results.

## Inhomogeneous Problem

### Impulse response - a particular solution

Eq. 89 represents the general solution for incoming waves reflected off the boundary in the fluid and outgoing waves in the elastic medium. We now calculate the impulse response and match specified boundary conditions to derive a particular solution. A dilatational impulsive source in a fluid filled borehole is a Hertzian oscillator $\frac{e^{ikR}}{R}$ (Brekhovskikh, 1960) which can be written in terms of the modified Bessel function $K_0(f'r)$ as follows (modified from Gradshteyn and Rhyzik, 1980, Eq. 6.677.5)

$$\frac{e^{ikR}}{R} = \int_{-\infty}^{\infty} K_0(f'r) e^{ik_z z} dk_z \tag{90}$$

This term is added to the fluid potential $\phi_f$ producing an inhomogeneous $\phi_f$

$$\phi_f = (K_0(f'r) + B_f I_0(f'r)) e^{-ik_z z} e^{i\omega t} \tag{91}$$

Boundary conditions are matched on the interface. The partial derivative operators (Eq. 5) from the boundary conditions commute with the double Fourier transform operator producing a system of linear equations.

### Solving for the boundary conditions

The boundary conditions are continuity of radial displacement, radial stress and vanishing of tangential stress. Had the inner medium been a solid instead of elastic then the latter boundary condition would have been continuity of tangential stress.

The continuity of the radial displacement boundary condition can be written

$$\begin{aligned} \frac{\partial \phi_f}{\partial r} &= \frac{\partial \phi}{\partial r} - \frac{\partial \psi'}{\partial z} \\ f' I_1(f'a) B_f - f' K_1(f'a) &= -l' K_1(l'a) A + i k_z K_1(m'a) C \end{aligned} \tag{92}$$

continuity of radial stress is written

$$\rho_f \frac{\partial^2 \phi_f}{\partial t^2} = \rho_b \frac{\partial^2 \phi}{\partial t^2} - 2\mu \left( \frac{1}{r} \frac{\partial \phi}{\partial r} + \frac{\partial^2 \phi}{\partial z^2} + \frac{\partial^2 \psi'}{\partial r \partial z} \right)$$

$$\begin{aligned} &-\rho_f \omega^2 \left[ I_0(f'a) B_f + K_0(f'a) \right] = \\ &\quad -\rho_b \omega^2 K_0(l'a) A - 2\mu \left( -\frac{l'}{a} K_1(l'a) - k_z^2 K_0(l'a) \right) A - 2\mu i k_z m' \left( K_0(m'a) + \frac{K_1(m'a)}{m'a} \right) C \end{aligned} \tag{93}$$

and vanishing of tangential stress is written

$$\rho_b \frac{\partial^2 \psi'}{\partial t^2} + 2\mu \left( \frac{\partial^2 \phi}{\partial r \partial z} - \frac{\partial^2 \psi'}{\partial z^2} \right) = 0$$

$$+ 2\mu i k_z l' K_1(l'r) A + \left( -\rho_b \omega^2 + 2\mu k_z^2 \right) K_1(m'a) C = 0. \tag{94}$$

### Use of Cramer's rule to solve the system

The boundary conditions form a $3 \times 3$ set of equations of the following form

$$\begin{vmatrix} b_{f1} & a_1 & c_1 \\ b_{f2} & a_2 & c_2 \\ b_{f3} & a_3 & c_3 \end{vmatrix} \begin{vmatrix} B_f \\ A \\ C \end{vmatrix} = \begin{vmatrix} g1 \\ g2 \\ g3 \end{vmatrix} \tag{95}$$

with the coefficient matrix from Eq. 92, Eq. 93, and Eq. 94.

$$\begin{vmatrix} f'I_1(f'a) & l'K_1(l'a) & -ik_zK_1(m'a) \\ \rho_f\omega^2 I_0(f'a) & \begin{matrix}(-\rho_b\omega^2+2\mu k_z^2)K_0(l'a)+\\ \frac{2\mu l'}{a}K_1(l'a)\end{matrix} & -2\mu ik_z m'\left(K_0(m'a)+\frac{K_1(m'a)}{m'a}\right) \\ 0 & +2\mu ik_z l'K_1(l'a) & (-\rho_b\omega^2+2\mu k_z^2)\,K_1(m'a) \end{vmatrix} \tag{96}$$

and the right hand side vector $g$

$$\begin{vmatrix} g_1 \\ g_2 \\ g_3 \end{vmatrix} = \begin{vmatrix} f'K_1(f'a) \\ -p_f\omega^2 K_0(f'a) \\ 0 \end{vmatrix}. \tag{97}$$

We will use Cramer's rule to solve for $B_f, A, C$. The Cramer's rule solution is the ratio of the determinant of each cofactor divided by the determinant of the coefficient matrix (Eq. 96). The determinant of the coefficient matrix can be written

$$b_{f1}a_2c_3 + b_{f2}a_3c_1 - (b_{f1}a_3c_2 + b_{f2}a_1c_3). \tag{98}$$

First we will calculate the $b_{f1}a_2c_3, b_{f1}a_3c_2$ terms with $I_1(f'a)$ in common

$$b_{f1}a_2c_3 = \tag{99}$$
$$\left[f'\left(-\rho_b\omega^2+2\mu k_z^2\right)^2 K_0(l'a)K_1(m'a) + \frac{2\mu l'f'}{a}(-\rho_b\omega^2+2\mu k_z^2)K_1(l'a)K_1(m'a)\right] I_1(f'a)$$
$$b_{f1}a_3c_2 = \tag{100}$$
$$4\mu^2 k_z^2 f\left[l'm'K_1(l'a)K_0(m'a) + \frac{l'K_1(l'a)K_1(m'a)}{a}\right] I_1(f'a).$$

Combining Eq. 99 and Eq. 100 and temporarily leaving off the common factor of $I_1(f'a)$ we get after some cancellation

$$f\left[\left(-\rho_b\omega^2+2\mu k_z^2\right)^2 K_0(l'a)K_1(m'a) - \frac{2\mu l'\omega^2\rho_b}{a}K_1(l'a)K_1(m'a) - 4\mu^2 k_z^2 l'm'K_1(l'a)K_0(m'a)\right]. \tag{101}$$

Following the same procedure for the $b_{f2}a_3c_1 - b_{f2}a_1c_3$ term

$$b_{f2}a_3c_1 - b_{f2}a_1c_3 = \rho_f\rho_b\omega^4 l'K_1(l'a)K_1(m'a)I_0(f'a). \tag{102}$$

We will now substitute the column vector $g_i$ for $b_{fi}$ in our matrix of coefficients and take the determinant of this cofactor to yield our Cramer's rule numerator. Since the

column vectors $b_{fi}, g_i$ are equivalent except the modified Bessel functions $K_0(f'a), K_1(f'a)$ replace $I_0(f'a), I_1(f'a)$, this numerator for calculating $B_f$ will have the same form as our denominator. If we do this replacement in our numerator and then divide both denominator and numerator by $K_1(l'a)K_1(m'a)$ we obtain

$$B_f = \frac{gK_1(f'a) - hK_0(f'a)}{gI_1(f'a) + hI_0(f'a)} \tag{103}$$

where from Eq. 102

$$h = \rho_f \rho_b \omega^4 l'$$

and from Eq. 101

$$g = f' \left[ \left( -\rho_b \omega^2 + 2\mu k_z^2 \right)^2 \frac{K_0(l'a)}{K_1(l'a)} - \frac{2\mu l' \rho_b \omega^2}{a} - 4\mu^2 k_z^2 l' m' \frac{K_0(m'a)}{K_1(m'a)} \right]. \tag{104}$$

To manipulate $g$ and $h$ into more recognizable forms we will go through a series of algebraic manipulations as follows

1. Divide through by $h$
2. Substitute $\frac{\omega}{c}$ for $k_z$, $\rho_b \beta^2$ for $\mu$
3. Collect terms.

Upon doing so we obtain

$$g = \frac{f' \rho_b}{l' \rho_f} \left[ \left( 2\frac{\beta^2}{c^2} - 1 \right)^2 \frac{K_0(l'a)}{K_1(l'a)} - \left( \frac{2\beta^2 l' m'}{\omega^2} \right) \left[ \frac{1}{m'a} + \frac{2\beta^2}{c^2} \frac{K_0(m'a)}{K_1(m'a)} \right] \right]. \tag{105}$$

$$h = 1$$

Eq. 105 is in a recognizable form from Cheng et al. (1982, Eq. A3) and Toksöz et al. (1984). For the solution of $B_f$ there has been no sign change by the use of $e^{i\omega t}$ dependence although the definition of the wavenumbers has changed, $f' = if$, etc.

We have solved for the coefficient governing wave propagation inside the borehole, $B_f$. The solution for $A$ and $C$ proceeds as follows. To solve for $A$ we have a new cofactor

$$\begin{vmatrix} f'I_1(f'a) & f'K_1(f'a) & -ik_z K_1(m'a) \\ \rho_f \omega^2 I_0(f'a) & -\rho_f \omega^2 K_0(f'a) & -2\mu i k_z m' \left( K_0(m'a) + \dfrac{K_1(m'a)}{a} \right) \\ 0 & 0 & \left( -\rho_b \omega^2 + 2\mu k_z^2 \right) K_1(m'a) \end{vmatrix}. \tag{106}$$

The determinant is our Cramer's rule numerator

$$-2f'\rho_f\omega^2(-\rho_b\omega^2+2\mu k_z^2)\left[K_0(f'a)I_1(f'a)+K_1(f'a)I_0(f'a)\right]K_1(m'a). \tag{107}$$

After applying the same sequence of transformations applied to the denominator we obtain

$$A=\frac{\dfrac{-2f'}{l'}\left(\dfrac{2\beta^2}{c^2}-1\right)\left[K_0(f'a)I_1(f'a)+K_1(f'a)I_0(f'a)\right]\dfrac{1}{K_1(l'a)}}{gI_1(f'a)+I_0(f'a)}. \tag{108}$$

For $C$ the cofactor is

$$\begin{vmatrix} f'I_1(f'a) & l'K_1(l'a) & f'K_1(f'a) \\ \rho_f\omega^2 I_0(f'a) & (-\rho_b\omega^2+2\mu k_z^2)K_0(l'a)+\dfrac{2\mu l'}{a}K_1(l'a) & -\rho_f\omega^2K_0(f'a) \\ 0 & +2\mu ik_z l'K_1(l'a) & 0 \end{vmatrix} \tag{109}$$

and proceeding as above we calculate the determinant of this matrix as our Cramer's rule numerator and apply the same sequence of tranformations to yield

$$C=\frac{\dfrac{+4if'\beta^2}{\omega c}\left[K_1(f'a)I_0(f'a)+I_1(f'a)K_0(f'a)\right]\dfrac{1}{K_1(m'a)}}{gI_1(f'a)+I_0(f'a)}. \tag{110}$$

A sign change has been introduced into $C$ by calculating it with $e^{i\omega t}$ positive time dependence instead of the $e^{-i\omega t}$ negative time dependence.

Both $A$ and $C$ are simplified considerably by utilizing the Wronskian (Abramowitz and Stegun, 1974, Eq. 9.6.15)

$$\left[K_1(f'a)I_0(f'a)+I_1(f'a)K_0(f'a)\right]=\frac{1}{f'a}$$

producing

$$A = \frac{\dfrac{-2}{l'a}\left(\dfrac{2\beta^2}{c^2}-1\right)\dfrac{1}{K_1(l'a)}}{gI_1(f'a)+I_0(f'a)} \tag{111}$$

$$C = \frac{\dfrac{4i\beta^2}{\omega ca}\dfrac{1}{K_1(m'a)}}{gI_1(f'a)+I_0(f'a)}. \tag{112}$$

In any Cramer's rule solution it is important to check the results. To check that $A$ and $C$ were correct we evaluated the vanishing of the tangential stress boundary

condition to yield a relationship between $A$ and $C$. The following relationship was obtained

$$A = \frac{-\omega c(\frac{2\beta^2}{c^2} - 1)}{2il'\beta^2} \frac{K_1(m'a)}{K_1(l'a)} C \tag{113}$$

and this relationship was satisfied by Eq. 111 and Eq. 112 giving confidence in the results. We substituted the new values of $A$ and $C$ into the third equation, vanishing of tangential stress, and achieved the sum of zero confirming the accuracy.

## Calculation of Radial and Vertical Displacement Fields

Recalling the displacement potential relations for axisymmetric media with the recoded $\psi$ (Eq. 18)

$$\begin{aligned} U_r &= \frac{\partial \phi}{\partial r} - \frac{\partial \psi'}{\partial z} \\ U_z &= \frac{\partial \phi}{\partial z} + \frac{\psi'}{r} + \frac{\partial \psi'}{\partial r} \end{aligned} \tag{114}$$

and carrying through with the differentiation using the differential identities (Eq. 5), we can rewrite the displacement components

$$\begin{aligned} U_r &= \int_{-\infty}^{\infty} \int_{-\infty}^{\infty} \left(-Al' K_1(l'r) + ik_z C K_1(m'r)\right) e^{-ik_z z} e^{i\omega t} d\omega dk_z \\ U_z &= \int_{-\infty}^{\infty} \int_{-\infty}^{\infty} \left(-ik_z A K_0(l'r) - m' C K_0(m'r)\right) e^{-ik_z z} e^{i\omega t} d\omega dk_z. \end{aligned} \tag{115}$$

The integral over $k_z$ is performed using the discrete wavenumber technique (Bouchon and Aki, 1977; Bouchon, 1981; Cheng and Toksöz, 1981; Dietrich et al., 1984) and the integral over $\omega$ is evaluated using a Fast Fourier Transform algorithm. A combination of factors applied to our integrals allows evaluation along the real axis using discrete wavenumber and FFT techniques. To lift all poles off the real axis when performing the discrete wavenumber integration over we introduce a small negative imaginary frequency $\omega_I$ component to our calculation (Bouchon and Aki, 1977). This component is removed in the time domain by multiplication by a factor $e^{\omega_I t}$. Attenuation is introduced through the use of complex velocities. The discrete wavenumber technique is explained more thoroughly in Appendix 1.

Utilizing the discrete wavenumber technique we can rewrite our integrals

$$U_r = \frac{2\pi}{L} \sum_{n=-\infty}^{\infty} \left(-Al' K_1(l'r) + ik_{zn} C K_1(m'r)\right) e^{-ik_{zn} z} \tag{116}$$

$$U_z = \frac{2\pi}{L} \sum_{n=-\infty}^{\infty} (-ik_{zn} A K_0(l'r) - m' C K_0(m'r)) e^{-ik_{zn} z} \tag{117}$$

where $k_{zn} = \frac{2\pi n}{L}$, $L$ equals the introduced periodicity of our medium, and for the sake of brevity the integral over $\omega$ was set aside.

An important simplification is warranted. It can be seen from our wavenumber relations that the radial wavenumbers $l', m', f'$ which are functions of $k_{zn}^2$ are even functions due to the squared $k_{zn}$ and therefore the modified Bessel functions $K, I$ are also even. $\alpha, \beta, a, \rho_f, \rho_b$ are all parameters so are identically positive. Neglecting these factors from our definitions of the coefficient $A, C$ (Eq. 111,Eq. 112) we can see that $A$ is an even function and $C$ is an odd function because of the dependence on $k_{zn}$ to the first power only.

In the sum of the radial component (Eq. 116) $U_r$, we can see that the $Al'K_1$ term is even and also that $ik_{zn}CK_1$ term is an odd function times an odd function yielding an even function. Thus the radial summation is even.

The converse is true for the sum of the vertical component (Eq. 117), we have $ik_{zn}AK_0$ or an odd function times an even function which is an odd function and $m'CK_0$ which is also an odd function.

Using arguments similar to those offered in Appendix 3 discussing even and odd integrals and their implications for Fourier analysis, we can use the evenness and oddness of the summands to halve our limits over the sum. We rewrite the sums using Euler's formula as (Eq. 116,Eq. 117)

$$U_r = \frac{2\pi}{L} \sum_{n=0}^{\infty} \varepsilon_n (-Al'K_1(l'r) + ik_{zn}CK_1(m'r)) \cos(-k_{zn} z) \tag{118}$$

$$U_z = \frac{2\pi}{L} \sum_{n=0}^{\infty} \varepsilon_n (-ik_{zn}AK_0(l'r) - m'CK_0(m'r)) i \sin(-k_{zn} z) \tag{119}$$

where $\varepsilon_n$ is the well known Neumann's factor equal to 1 at $n = 0$ and equal to 2 at $n \neq 0$.

## Synthetic microseismograms

We now show example seismograms generated with the discrete wavenumber technique and later show tests of its reliability. Three different sets of density and velocity parameters were used from common lithologies - a sand, shale and limestone. The lithologies are a Pierre shale (Thomsen, 1986, after White, 1982) representative of a generally low velocity material, a Berea sandstone (Thomsen, 1986, after King, 1964)

representative of a well-cemented sandstone with low Poisson's ratio and a Solenhofen limestone (Press, 1986 after Hughes and Cross, 1951) representative of a hard micritic limestone. Table 1. shows the properties of these three lithologies.

Figure 5 shows the geometry of the source and receiver array. The source is centered on the axis of the borehole and is a volume dilatational source. A vertical point receiver array is placed outside the borehole a distance of either 1 or 5 m. The height of the receiver array is respectively 1 and 5 m with 6 equally spaced receivers spread throughout. The radius of the borehole is .1 m, approximating an 8 inch diameter borehole.

The impulse response from the discrete wavenumber technique is convolved with a Ricker Wavelet with a center frequency of 1500 Hz and a later example will show a convolution at a lower frequency. The form of the Ricker wavelet used is $\frac{\omega^2}{\omega_c^2} e^{-\frac{\omega^2}{\omega_c^2}}$ where $\omega_c$ is the center frequency. A constant time shift was applied to the Ricker wavelets. The Q is 100 for both $P$ and $S$.

Figure 6 shows the radial and vertical components of radiation from a source in Pierre shale at 1500 Hz frequency for the wavelet. The source-vertical receiver array separation is 1m. It was characteristic for the Pierre Shale seismograms to have equal peak amplitudes in both the radial and vertical components. Since the vertical component is odd with respect to the horizontal axis, the vertical component amplitude is 0 on this axis. Thus the bottom seismogram of the vertical components plots as a straight line. Moreover, it can be readily seen that the $P$ wave motion becomes more vertical and the $S$ wave motion more horizontal proceeding up the array. Figure 7 shows the radial and vertical components of radiation from a source in Berea sandstone at 1500 Hz. Figure 8 shows the radial and vertical components for a source in Solenhofen limestone at 1500 Hz and shows similiarities to the Berea sandstone (Figure 7) which has similarly high velocities and very little separation between $P$ and $S$.

The discrete wavenumber formulation presented here does not include the effects of porosity and thus no fluid motion of the tube wave is considered. It is nonetheless interesting that no visible tube wave arrival or effect can be discerned 1m away from the borehole.

Figure 9 shows the same radial and vertical components but for a source-receiver separation of 5m in Pierre shale. Note the time scale change. Figure 10 similarly shows the radial and vertical components for a source-receiver separation of 5m in Berea sandstone. Figure 11 shows the radial and vertical components for the same source-receiver geometry in Solenhofen limestone. It is evident that amplitudes are decreasing in the distance from 1m to 5m as would be expected. However, the relative amplitudes of horizontal to vertical components are changing. There is another observation at 5m

which might be indicative of the development of the far-field $P$ radiation pattern. The Berea sandstone has a very low Poisson's ratio $\sigma = .17$ which means that the tops of the peanut-shaped P-wave radiation pattern will be depressed, more peanut-shaped. Therefore the relative vertical component will be less than the radial component. This is something we can begin to see in the near field.

### Test of the technique

Since applying the discrete wavenumber technique to radiation outside the borehole was a new procedure, a few rudimentary tests were run to test the stability of the technique. Of course, these tests will indicate if the technique is definitely wrong but if passed do not represent conclusive proof that the technique is correct. As mentioned before, the algebra was shown to satisfy Cramer's rule and the relationship between the constants $A$ and $C$ was shown to satisfy the vanishing of the tangential stress boundary condition. The next test run was to vary the discretization length $L$. Figure 12 shows the radial component of a source in a fluid-filled borehole surrounded by Pierre shale with a source-receiver array separation of 1 m for two different discretization lengths, $L$=10.0 m and $L$=12.0 m. There is less than a .2% discrepancy in amplitude in this case. The equivalence shows that even with the two discretization lengths indicating sampling of $k_z$ space at different points, the results are equivalent.

### Frequency Dependence

A brief test of the frequency-amplitude effects was undertaken. Figure 13 shows waveforms for a source-receiver separation of 5 m in Pierre shale with two different frequency contents. Figure 14 has the same geometry and frequency dependences as Figure 13 but for a Berea sandstone. It can be seen that the amplitude of the Pierre shale seismograms increases relative to the Berea as the frequency decreases. The Pierre shale amplitude for low frequency is 1.6 units versus the 1.3 units for the Berea, a trend opposite to that for the 1.5 kHz case. This is because the high frequencies which are attenuated more readily in the Pierre shale have less effect on the low frequency results.

## CONCLUSIONS

An introduction to radiation from downhole sources has been presented in this paper. A literature review, review of the fundamental mathematics of source description and a description of the discrete wavenumber technique applied to the radiation from borehole problems was described in this paper. The discrete wavenumber technique provided a fast way to study radiation from a borehole source. It was found that with

Velocities and Densities of Three Common Lithologies and Steel

| Lithology/Property | $V_p$ | $V_s$ | $\sigma$ | $\rho$ |
|---|---|---|---|---|
| Solenhofen limestone | 5,970 (19,582) | 2,880 ( 9,446) | .308 | 2.656 |
| Berea sandstone | 4,206 (13,796) | 2,664 ( 8,738) | .165 | 2.140 |
| Pierre shale | 2,074 ( 6,803) | 869 ( 2,850) | .394 | 2.25 |
| Steel, 1%C | 5,854 (19,201) | 3,150 (10,332) | .308 | 7.854 |

Table 1: Velocities and densities of three common lithologies that are used in this paper. Velocities in $m/sec$ $(ft/sec)$, densities in $g/cm^3$, $\sigma$ is Poisson's ratio.

$Q$ of 100, the amplitudes of the waveforms from a point source in a fluid-filled borehole surrounded by Pierre shale are similar to those of a source borehole surrounded by hard Berea sandstone and Solenhofen limestone. However, radiation pattern theory explored in part two would predict much higher peak amplitudes in Pierre shale. A second conclusion is that amplitudes are substantially affected by the frequency content of the waveforms. For instance the $P$ wave is more energetic relative to the $S$ wave at higher frequencies. A third conclusion is that even in the near field we can begin to see the development of displacement patterns which abide by the far-field radiation patterns. Finally, the discrete wavenumber technique is stable and we are confident that it can be applied profitably to the description of downhole seismic sources.

## ACKNOWLEDGEMENTS

This work was supported by the Full Waveform Acoustic Logging Consortium at M.I.T. We would like to thank Jim DiSiena of Arco and Benoit Paternoster of Elf-Aquitaine for being particularly influential in the adoption of the topic of source description theory as presented in these papers.

## REFERENCES

Abo-Zena, A., Radiation from a finite cylindrical explosive source, *Geophysics, 42,* 1384–1393, 1977.

Aki, K. and K. L. Larner, Surface motion of a layered medium having an irregular interface due to incident plane Sh waves, *J. Geophys. Res., 1975,* 933–954, 1970.

Aki, K. and P. Richards, *Quantitative seismology: theory and methods,* vol. I,II, W.H. Freeman and Co., 1980.

Baker, L. and G. Winbow, Multipole logging in invaded formations, in *SEG Annual Meeting Expanded Technical Program Abstracts,* 1985.

Balch, A. and M. Lee, *Vertical Seismic Profiling Technique, Applications, and Case Histories,* D. Reidel Publishing Co., 1984, Chapter 5.

Bard, P. and M. Bouchon, The seismic response of sediment-filled valleys. part 1. the case of incident Sh waves, *Bull. Seis. Soc. Am., 70,* 1263–1286, 1980a.

Bard, P. and M. Bouchon, The seismic response of sediment-filled valleys. part 2. the case of incident P and Sv waves, *Bull. Seis. Soc. Am., 70,* 1921–1941, 1980b.

Ben-Menahem, A. and S. Singh, *Seismic Waves and Sources,* Springer-Verlag, 1981.

Beydoun, W., *Sources of seismic noise in boreholes,* Master's thesis, Mass. Inst. of Tech., 1982.

Beydoun, W., Seismic tool-formation coupling in boreholes, in *Vertical Seismic Profiling part B:Advanced Concepts,* edited by M. N. Toksöz and R. R. Stewart, Geophysical Press, 1984.

Biot, M., Propagation of elastic waves in a cylindrical bore containing a fluid, *J. App. Phys., 23,* 997–1009, 1952.

Biot, M., Theory of elastic waves in a fluid-saturated porous solid, II. higher frequency range, *J. Acoust. Soc. Am., 28,* 179–191, 1956a.

Biot, M., Theory of propagation of elastic waves in a fluid saturated porous solid, I. lower frequency range, *J. Acoust. Soc. Am., 28,* 168–178, 1956b.

Bouchon, M., A simple method to calculate Green's functions for elastic layered media, *Bull. Seis. Soc. Am., 71,* 959–971, 1981.

Bouchon, M. and K. Aki, Discrete wave-number representation of seismic-source wave fields, *Bull. Seis. Soc. Am., 67,* 259–277, 1977.

Bouchon, M., M. Campillo, and S. Gaffet, A boundary integral equation-discrete wavenumber representation method to study wave propagation in multilayered media having irregular interfaces, *Geophysics, 54,* 1134–1140, 1989.

Bowman, F., *Introduction to Bessel functions,* Dover Publications, Inc., 1958.

Brekhovskikh, L. M., *Waves in Layered Media,* Academic Press, first edition, 1960.

Campillo, M. and M. Bouchon, Synthetic Sh-seismograms in a laterally varying medium by the discrete wavenumber method, *Geophys. J. Royal Astr. Soc., 82,* 307–317, 1985.

Cheng, C. and M. Toksöz, Elastic wave propagation in a fluid-filled borehole and synthetic acoustic logs, *Geophysics, 46,* 1042–1053, 1981.

Cheng, C. and M. Toksöz, Generation, propagation and analysis of tube waves in a borehole, in *Vertical Seismic Profiling part B: advanced concepts,* edited by M. N. Toksöz and R. R. Stewart, Geophysical Press, 1984.

Cheng, C., M. Toksöz, and M. Willis, Determination of in-situ attenuation from full waveform acoustic logs, *J. Geophys. Res., 87,* 5477–5484, 1982.

Cicerone, R., J. Lee, M. Toksöz, and S. Alexander, Fracture detection and characterization from hydrophone VSP data, Kent Cliffs, New York, 1988, Reservoir Delineation Consortium Annual Report.

Ewing, W., W. Jardetzky, and F. Press, *Elastic waves in layered media,* McGraw-Hill, 1957.

Fehler, M. and C. Pearson, Acoustic radiation patterns for borehole sources, in *Trans., Soc. Prof. Well Log Anal.,* 1981, paper MM.

Fehler, M. and C. Pearson, Cross-hole seismic surveys: applications for studying subsurface fracture systems at a hot dry rock geothermal site, *Geophysics, 49,* 37–45, 1984.

Gradshteyn, I. and I. Ryzhik, *Table of integrals, series, and products,* Academic Press, corrected and enlarged by A. Jeffreys edition, 1980.

Greenfield, R. J., Seismic radiation from a point source on the surface of a cylindrical cavity, *Geophysics, 43,* 1071–1082, 1978.

Harkrider, D., Surface waves in multilayered elastic media 1. Rayleigh and Love waves from buried sources in a multilayered elastic half-space, *Bull. Seis. Soc. Am., 54,* 627–679, 1964.

Hazebroek, P., Elastic waves from a finite line source, *Proc. Roy. Soc. London, 294A,* 38–65, 1966.

Heelan, P., *The theory of head wave propagation along a plane interface separating two solid media,* PhD thesis, University of St. Louis, 1952.

Heelan, P., On the theory of head waves, *Geophysics, 18,* 871–893, 1953a.

Heelan, P., Radiation from a cylindrical source of finite length, *Geophysics, 18,* 685–696, 1953b.

Hughes, D. and J. Cross, Elastic wave velocities in rocks, *Geophysics, 16,* 577–593, 1951.

Jordan, D., The stress wave from a finite, cylindrical explosive source, *J. Math. Mech., 11,* 503–551, 1962.

Kennedy, W., W. Wiggins, and P. Aronstam, Swept-frequency borehole source for inverse VSP and cross-borehole surveying, in *SEG Annual Meeting Expanded Technical Program Abstracts,* 1988.

Kennett, B., *Seismic wave propagation in stratified media,* Cambridge University Press, 1983.

Kitsunezaki, C., A new method for shear-wave logging, *Geophysics, 45,* 1489–1506, 1980.

Kurkjian, A., Numerical computation of individual far-field arrivals excited by an acoustic source in a borehole, *Geophysics, 50,* 852–866, 1985.

Kurkjian, A., Theoretical far-field radiation from a low-frequency horizontal acoustic point force in a vertical borehole, *Geophysics, 51,* 930–939, 1986.

Kurkjian, A. and S. Chang, Acoustic multipole sources in fluid-filled boreholes, *Geophysics, 51,* 148–163, 1986.

Lee, M., *Scattered waves on the wall of a fluid-filled borehole from incident plane waves,* Open-File Report 85-666, U.S.G.S, 1985a.

Lee, M., *Two and three-dimensional low-frequency radiation from an arbitrary source in a fluid-filled borehole,* Open-File Report 85-550, U.S.G.S, 1985b.

Lee, M., Low-frequency radiation from point sources in a fluid-filled borehole, *Geophysics, 49,* 27–36, 1986.

Lee, M. and A. Balch, Theoretical seismic wave radiation from a fluid-filled borehole, *Geophysics, 47,* 1308–1314, 1982.

Lee, M., A. Balch, and K. Parrot, Radiation from a downhole airgun source, *Geophysics, 49,* 27–36, 1984.

Lo, T., M. Toksöz, S. Xu, and R. Wu, Ultrasonic laboratory tests of geophysical tomographic reconstruction, *Geophysics, 53,* 947–956, 1988.

Love, A., *A treatise on the mathematical theory of elasticity,* Dover, fourth edition, 1927.

Malvern, L. E., *Introduction to the mechanics of a continuous medium,* Prentice-Hall, 1969.

Miklowitz, J., *The theory of elastic waves and waveguides,* North-Holland Publishing Co., 1978.

Morse, P. and H. Feshbach, *Methods of theoretical physics, Volume I and II,* McGraw-Hill Book Co., 1953.

Owen, T., W. Balogh, and W. Peters, Arc discharge pulse source for borehole seismic applications, in *SEG Annual Meeting Expanded Technical Program Abstracts,* 1988.

Pao, Y. and C. Mow, *Diffraction of elastic waves and dynamic stress concentrations,* Crane, Russack and Co., Inc., 1971.

Pardo-Casas, F., C. Cheng, and R. Stephen, The study of wave propagation in a borehole using the finite difference method, in *SEG Annual Meeting Expanded Technical Program Abstracts,* 1984.

Paulsson, B. N., Three-component downhole seismic vibrator, in *SEG Annual Meeting Expanded Technical Program Abstracts,* 1988.

Peterson, E., Acoustic wave propagation along a fluid-filled cylinder, *J. App. Phys., 45,* 3340–3350, 1974.

Pilant, W. L., *Elastic waves in the Earth,* Elsevier, 1979.

Press, W., B. Flannery, S. Teukolsky, and W. Vettering, *Numerical recipes-the art of scientific computing,* Cambridge Univ. Press, 1986.

Rayleigh, J., On the dynamical theory of gratings, *Proc. Lond. Math. Soc., A79,* 399–416, 1907.

Roever, W., J. Rosenbaum, and T. Vining, Acoustic waves from an impulsive source in a fluid-filled borehole, *J. Acoust. Soc. Am., 55,* 1144–1157, 1974.

Rosenbaum, J., Synthetic microseismograms: logging in porous formations, *Geophysics, 39,* 14–32, 1974.

Schey, H., *Div, Grad, Curl, and All That: An Informal Text on Vector Calculus,* W.W. Norton and Co., 1973.

Schmitt, D. and M. Bouchon, Full wave acoustic logging-synthetic microseismograms and frequency-wavenumber analysis, *Geophysics, 50,* 1756–1778, 1985.

Schmitt, D., M. Bouchon, and G. Bonnet, Full wave synthetic acoustic logs in radially semiinfinite saturated porous media, *Geophysics, 53,* 807–823, 1988.

Schoenberg, M., Fluid and solid motion in the neighborhood of a fluid-filled borehole due to the passage of a low-frequency elastic plane wave, *Geophysics, 51,* 1191–1205, 1986.

Schoenberg, M., T. Marzetta, J. Aron, and R. Porter, Space-time dependence of acoustic waves in a borehole, *J. Acoust. Soc. Am., 70,* 1496–1507, 1981.

Siggins, A., *Circulating elastic waves on boreholes and cavities,* PhD thesis, The University of New England, 1989.

Siggins, A. and A. Stokes, Circumferential propagation of elastic waves on boreholes and cylindrical cavites, *Geophysics, 52,* 514–529, 1987.

Stephen, R., F. Pardo-Casas, and C. Cheng, Finite difference synthetic acoustic logs, *Geophysics, 50,* 1588–1609, 1985.

Tang, X. and C. Cheng, A dynamic model for fluid flow in open borehole fractures, *J. Geophys. Res., 94,* 7567–7576, 1989.

Thomsen, L., Weak elastic anisotropy, *Geophysics, 51,* 1954–1966, 1986.

Toksöz, M., C. Cheng, and M. Willis, Seismic waves in a borehole - a review, in *Vertical Seismic Profiling part B: advanced concepts,* edited by M. N. Toksöz and R. R. Stewart, Geophysical Press, 1984.

Tongtaow, C., *Wave propagation along a cylindrical borehole in a transversely isotropic medium,* PhD thesis, Colorado School of Mines, 1982.

Tsang, L. and J. Kong, Asymptotic methods for the first compressional head wave arrival in a fluid-filled borehole, *J. Acoust. Soc. Am., 65,* 647–654, 1979.

Tsang, L. and D. Rader, Numerical evaluation of the transient acoustic waveform due to a point source in a fluid-filled borehole, *Geophysics, 44,* 1706–1720, 1979.

Tubman, K., *Full waveform acoustic logs in radially layered boreholes,* PhD thesis, Mass. Inst. of Tech., 1984.

Tubman, K., C. Cheng, and M. Toksöz, Synthetic full-waveform acoustic logs in cased boreholes, *Geophysics, 49,* 1051–1059, 1984a.

Tubman, K., S. Cole, C. Cheng, and M. Toksöz, Dispersion curves and synthetic microseismograms in unbonded cased boreholes, in *M.I.T. Full Waveform Acoust. Logging Cons. Rept.,* 1984b.

Tubman, K., C. Cheng, S. Cole, and M. Toksöz, Synthetic full waveform acoustic logs in cased boreholes II. poorly bonded casing, *Geophysics, 51,* 902–913., 1986.

Viktorov, I., Rayleigh waves on a cylindrical surface, *Soviet Phys. Acoust., 4,* 131–136, 1958.

White, J., Signals in a borehole due to plane waves in the solid, *J. Acoust. Soc. Am., 25,* 906–915, 1953.

White, J., Use of reciprocity theorem for computation of low-frequency radiation patterns, *Geophysics, 25,* 613–624, 1960.

White, J., Elastic waves along a cylindrical bore, *Geophysics, 27,* 327–333, 1962.

White, J., *Seismic waves, radiation, transmission and attenuation,* McGraw-Hill Co., 1965.

White, J., *Underground sound: application of seismic waves,* Elsevier, 1983.

White, J. and R. Sengbush, Shear wave from explosive sources, *Geophysics, 28,* 1101–1119, 1963.

White, J. and C. Tongtaow, Cylindrical waves in transversely isotropic media, *J. Acoust. Soc. Am., 70,* 1496–1507, 1981.

White, J. and R. Zechman, Computed response of an acoustic logging tool, *Geophysics, 33,* 302–310, 1968.

White, J., I. Martineau-Nicoletis, and C. Monash, Measured anisotropy in Pierre Shale, *Geophys. Prosp., 31,* 709–725, 1982.

Winbow, G., Compressional and shear arrivals in a multipole sonic log, *Geophysics, 50,* 1119–1126, 1985.

Wu, R. and M. Toksöz, Diffraction tomography and multisource holography applied to seismic imaging, *Geophysics, 52,* 11–25, 1987.

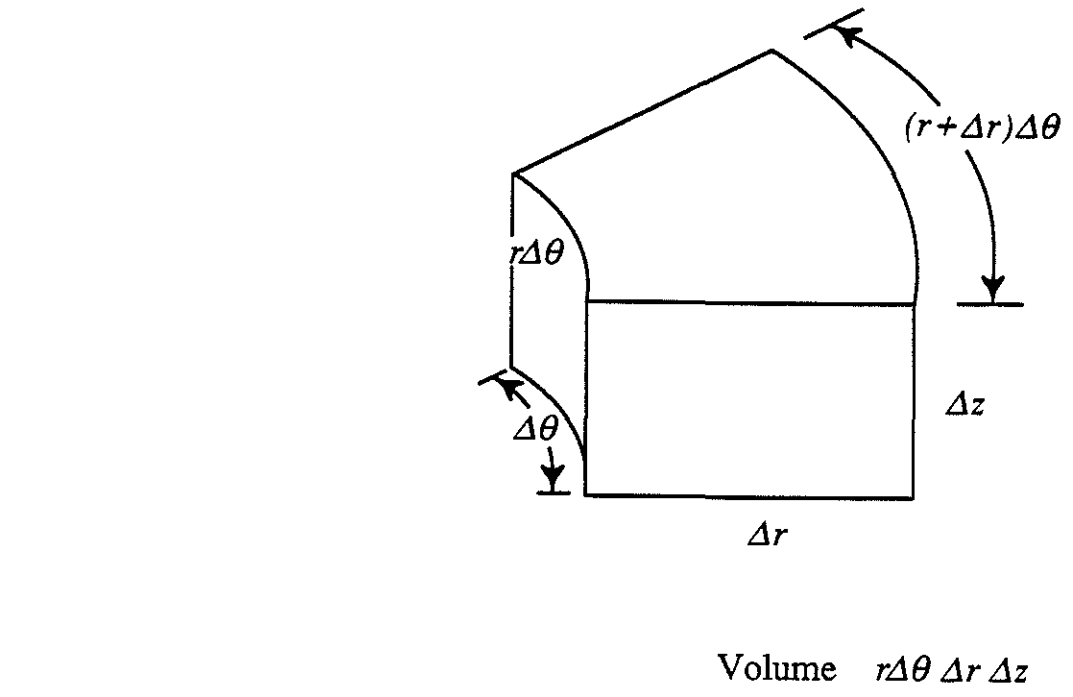


Figure 1: Elementary cylindrical element. Elongation of the chord in the radial direction is shown.

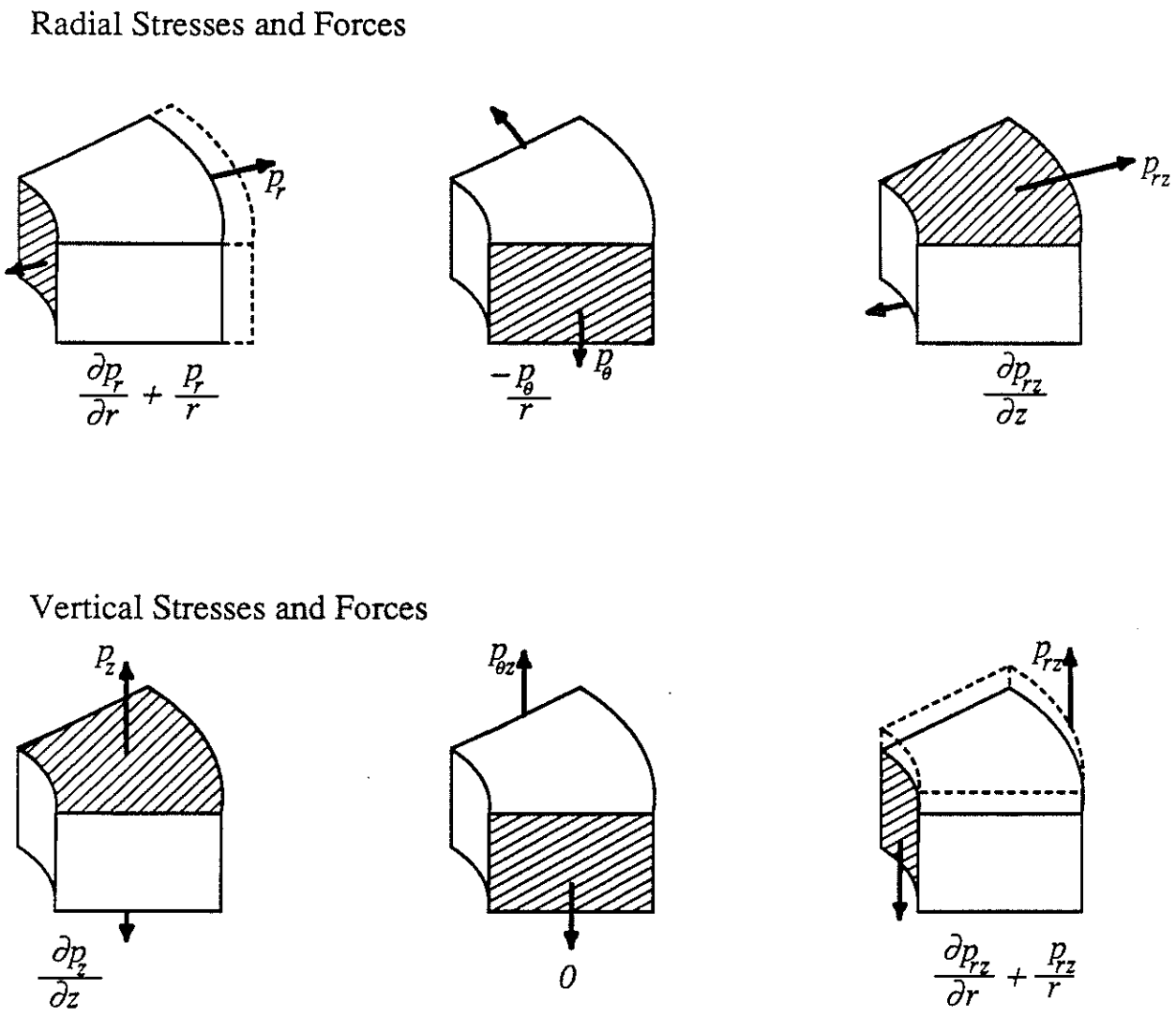


Figure 2: This figure shows the stresses and forces for axisymmetric wave propagation over an elementary cylindrical element. Stresses are indicated by arrows. Resulting forces indicated below each element.

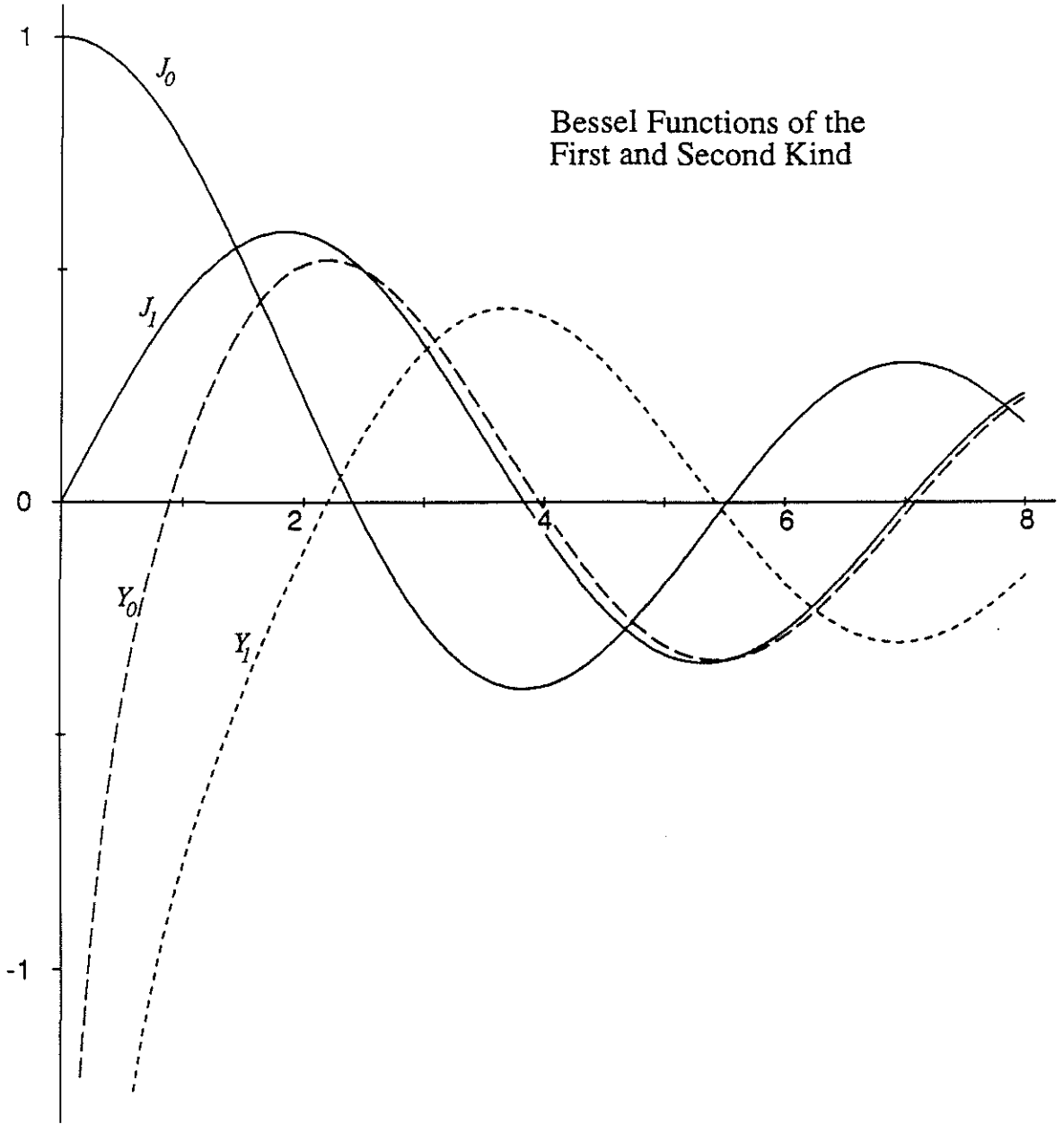


Figure 3: Zeroth and first order Bessel functions of the first and second kind. Computed from a program in Press et al., 1986. The behavior of both $J_n$ and $Y_n$ mimic a sinusoidal decaying exponential.

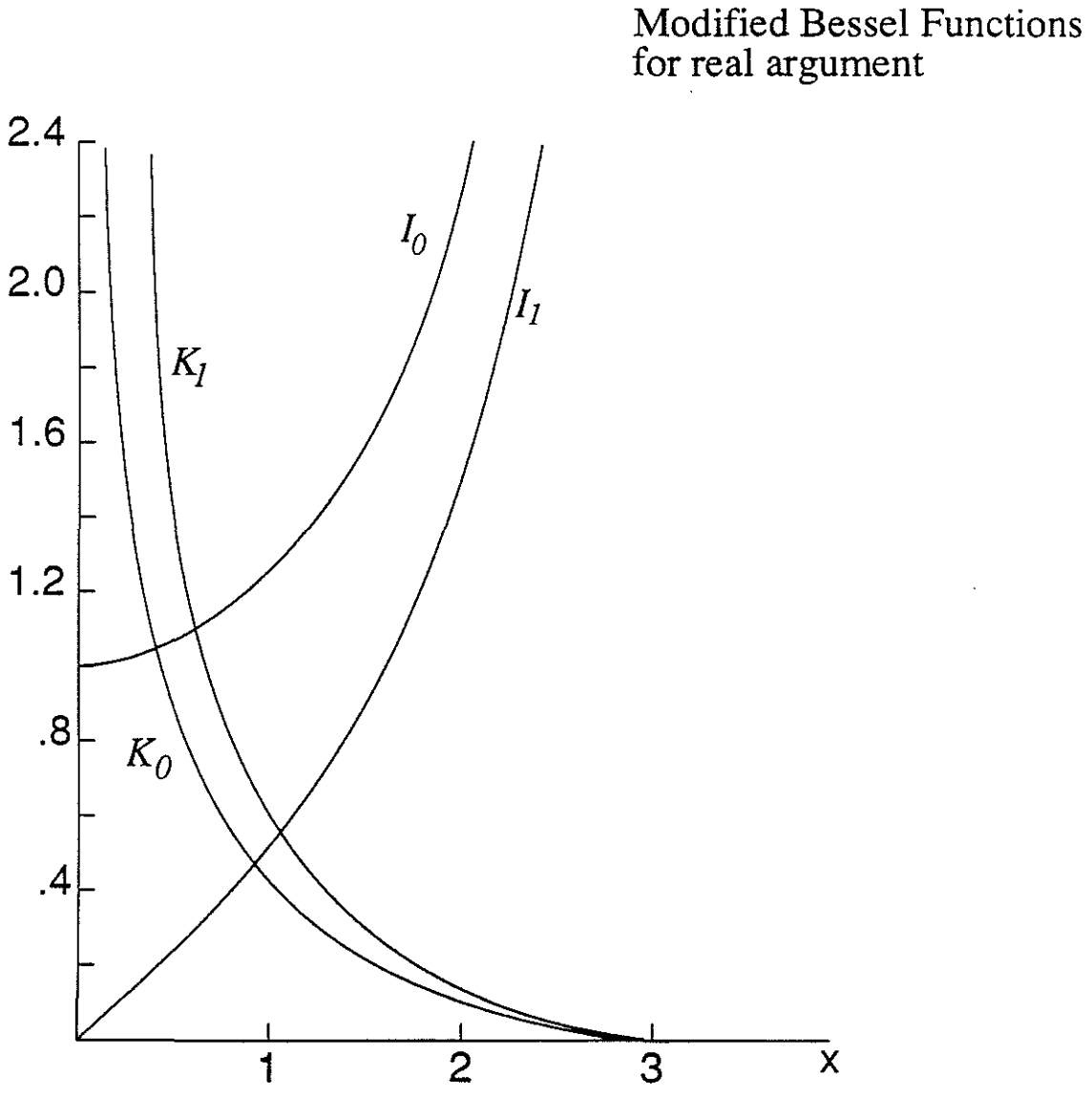


Figure 4: After Abramowitz and Stegun (1964). Behavior of modified Bessel functions of orders zero and one for real argument. The exponentially decreasing nature of $K_{0,1}$ and the exponentially increasing nature of $I_{0,1}$ is clearly seen.

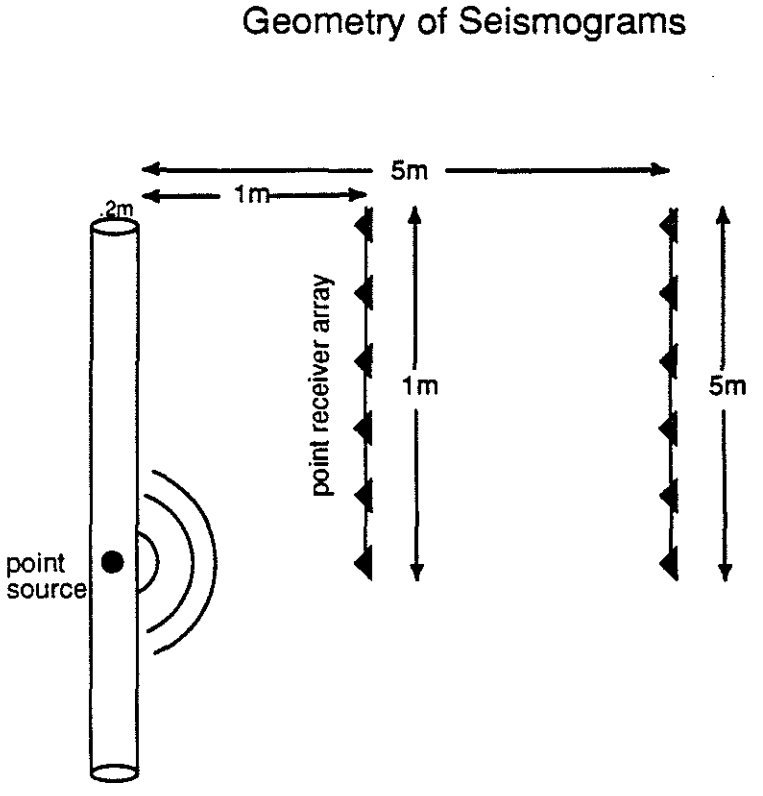


Figure 5: Geometry of the synthetic seismograms. Point source is placed in fluid-filled borehole and receiver arrays are spaced 1 and 5 m apart.

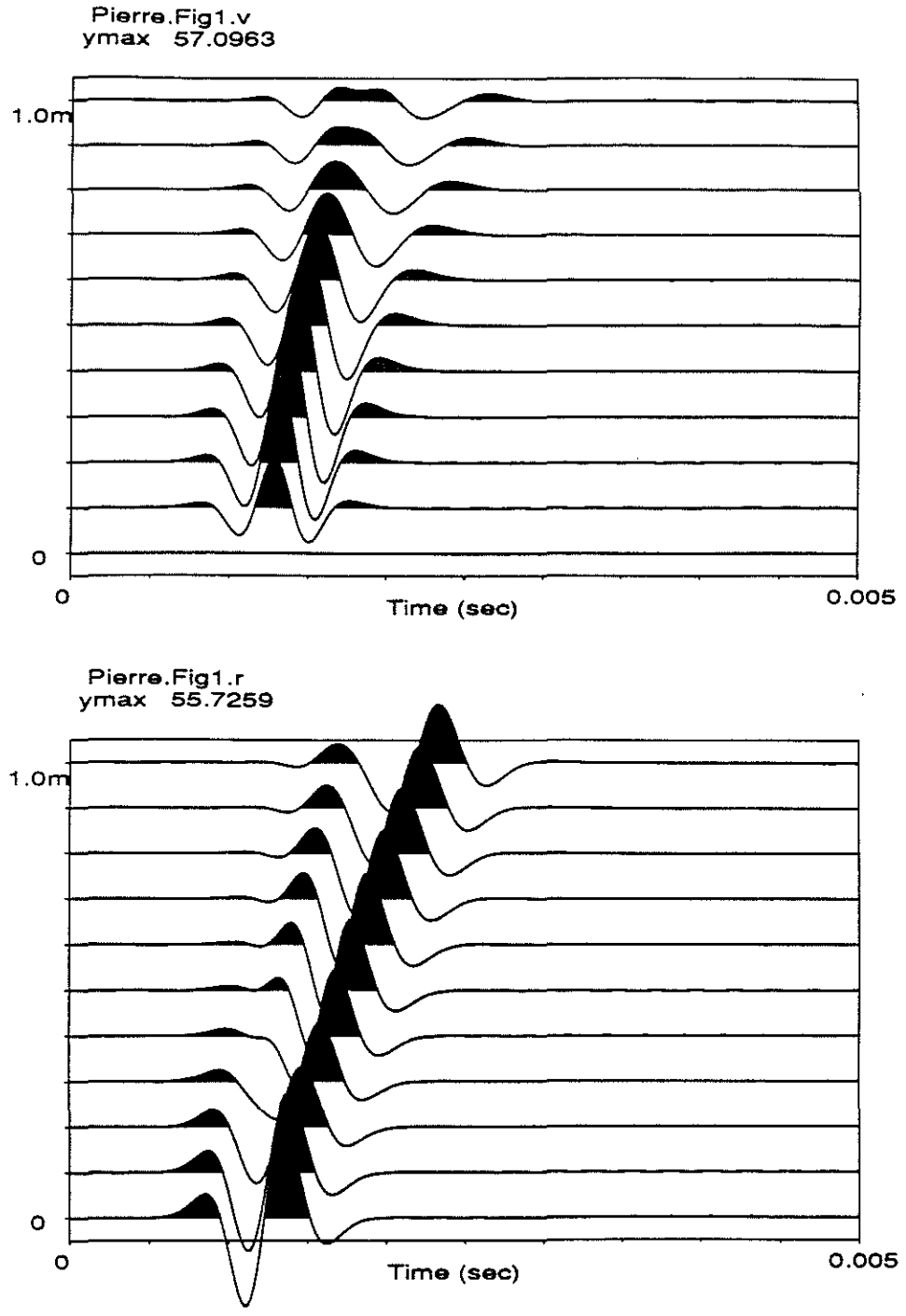


Figure 6: Vertical (top) and radial (bottom) component seismograms. Geometry is presented in Figure 5 and represents source in a fluid filled borehole surrounded by Pierre shale. 1m source-receiver array distance. 1500 Hz Ricker wavelet

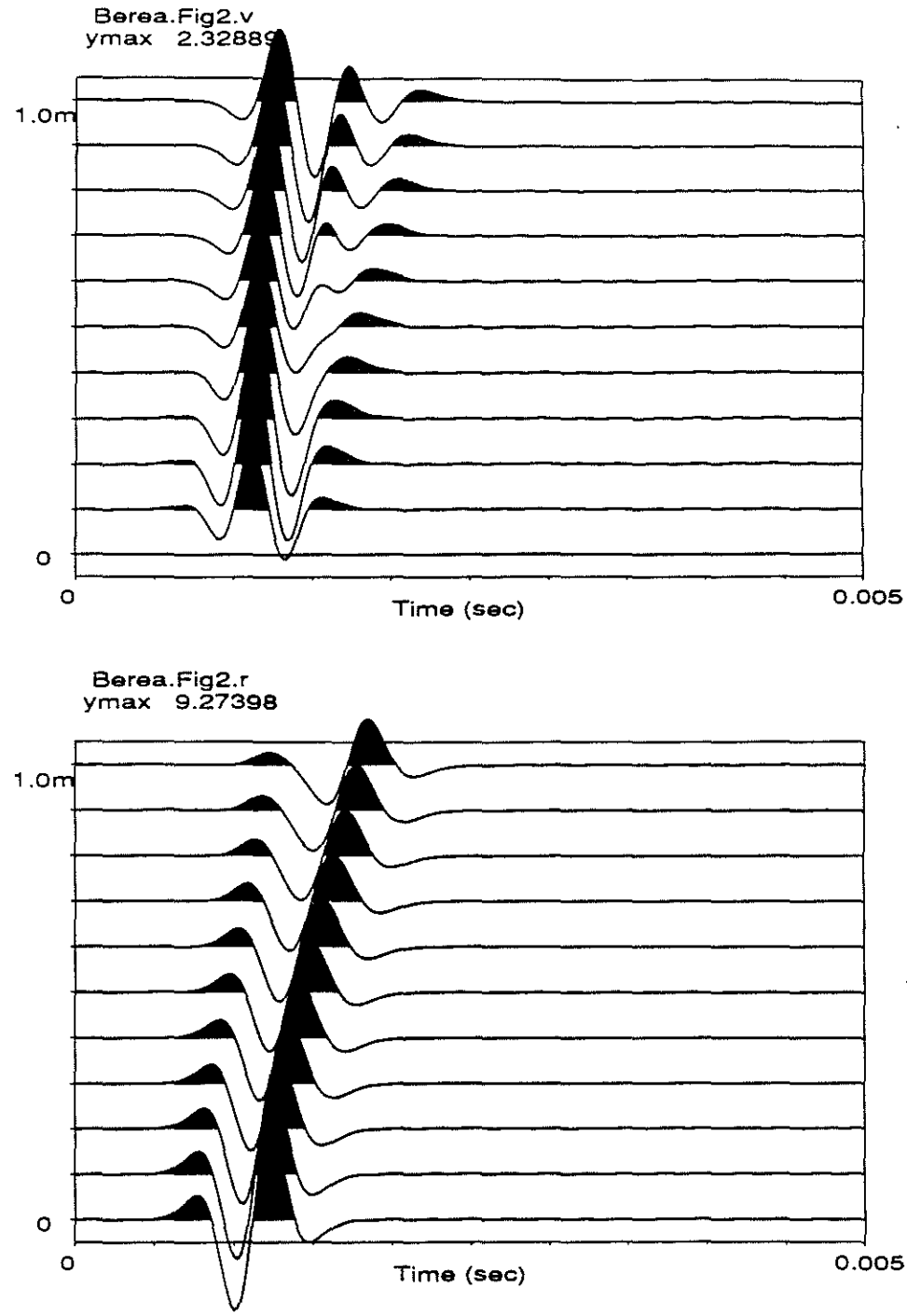


Figure 7: Vertical (top) and radial (bottom) component seismograms. Lithology is Berea sandstone. Distance vertical array is away from source is 1 m.

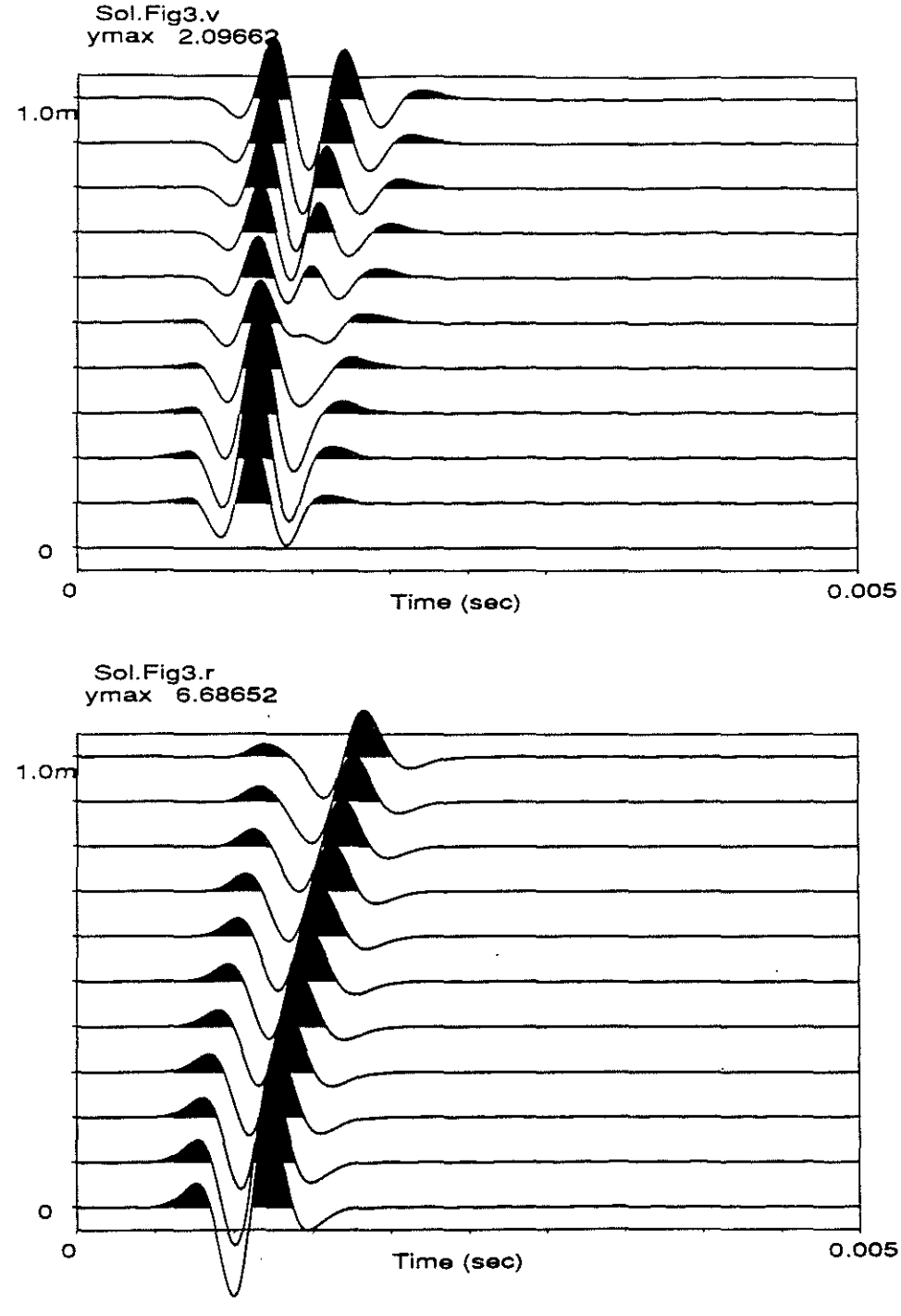


Figure 8: Vertical (top) and radial (bottom) component seismograms. Lithology is Solenhofen limestone. Distance vertical array is away from source is 1 m.

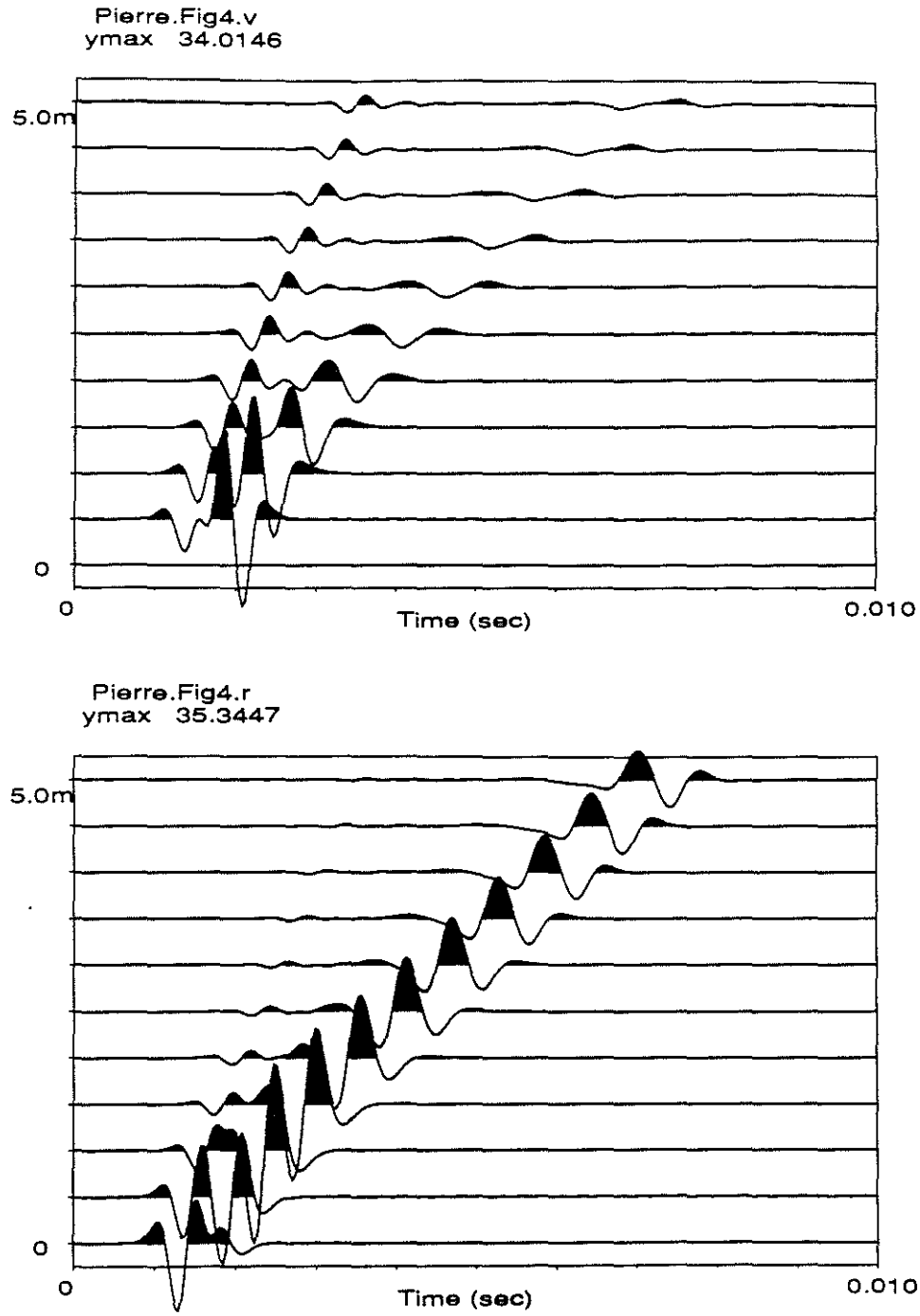


Figure 9: Vertical (top) and radial (bottom) component seismograms. Lithology is Pierre shale. Distance vertical array is away from source is 5 m.

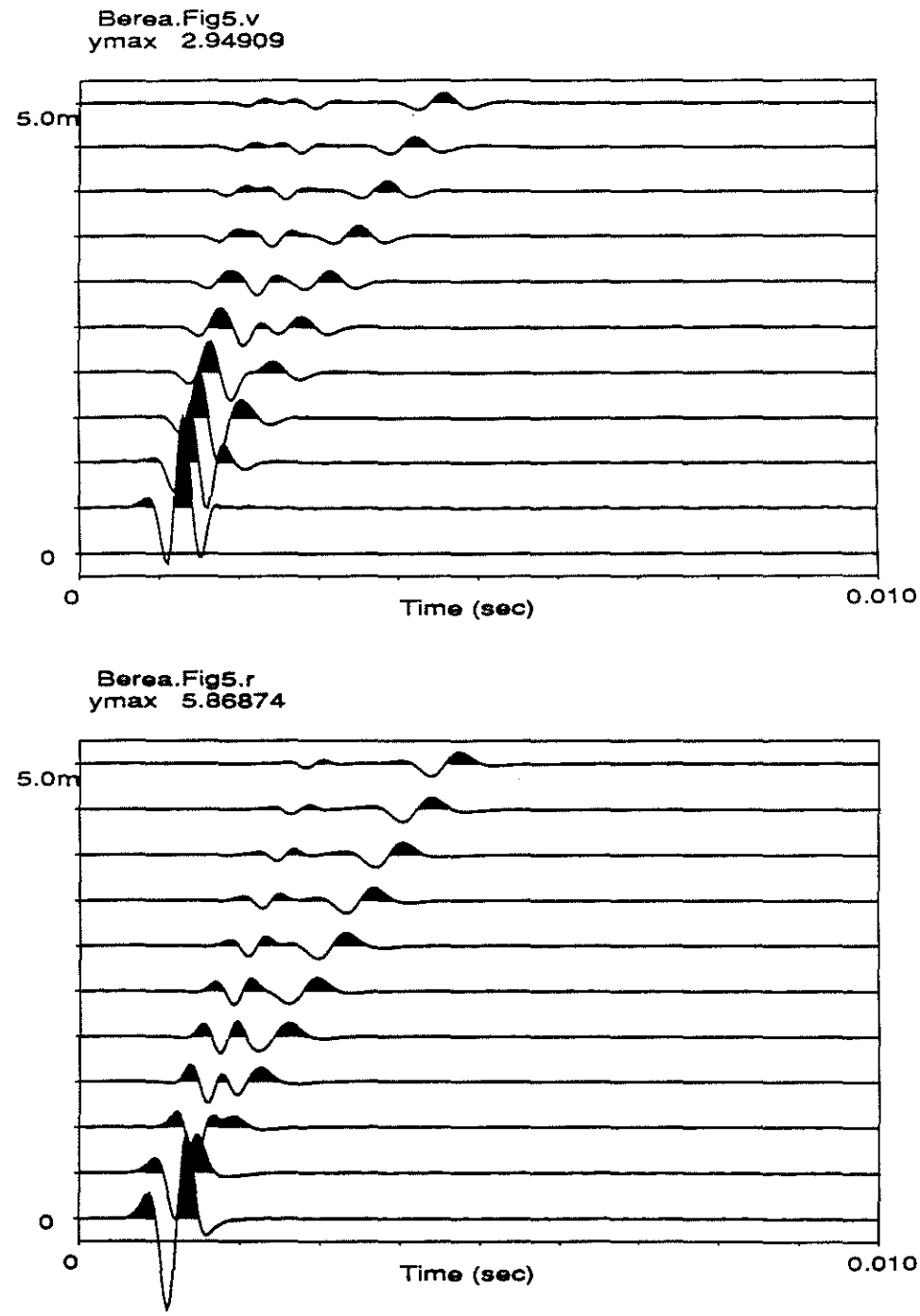


Figure 10: Vertical (top) and radial (bottom) component seismograms. Lithology is Berea sandstone. Distance vertical array is away from source is 5 m.

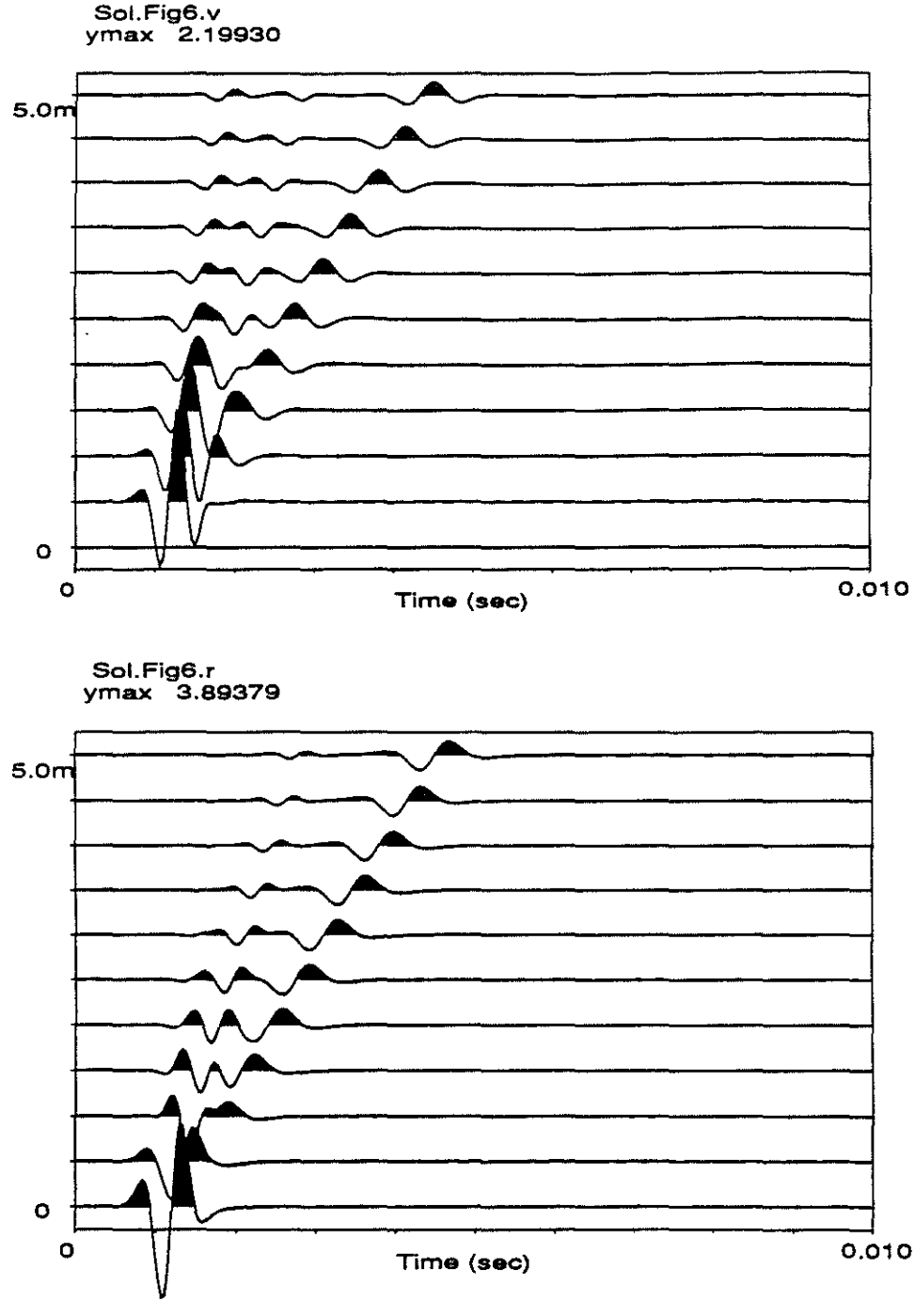


Figure 11: Vertical (top) and radial (bottom) component seismograms. Lithology is Solenhofen limestone. Distance vertical array is away from source is 5 m.

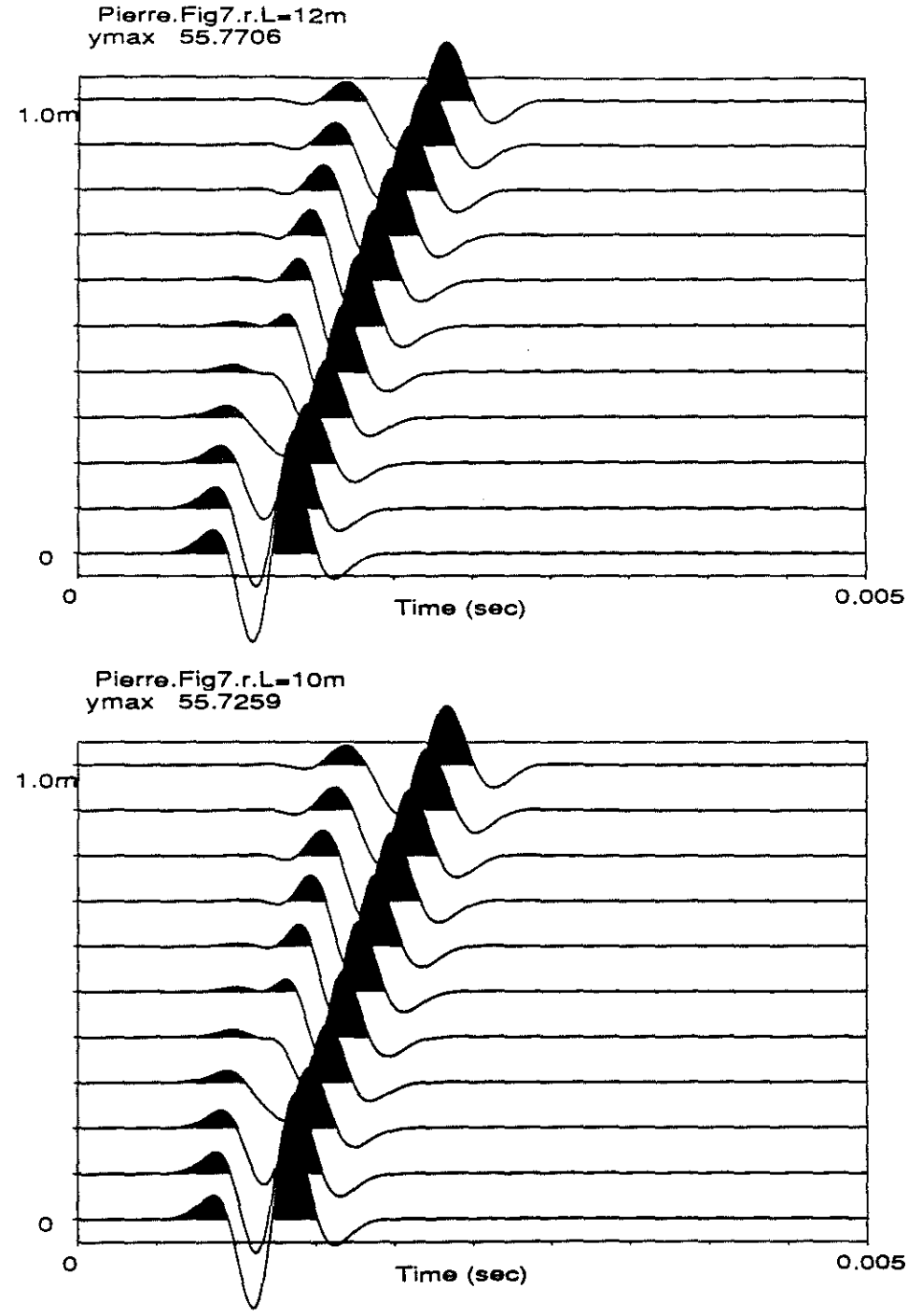


Figure 12: This figure shows a test of the program. Variation of discretization length from 10 to 12 m produces no change in output waveforms, lithology is Pierre shale. Vertical receiver array 1 m away from borehole.

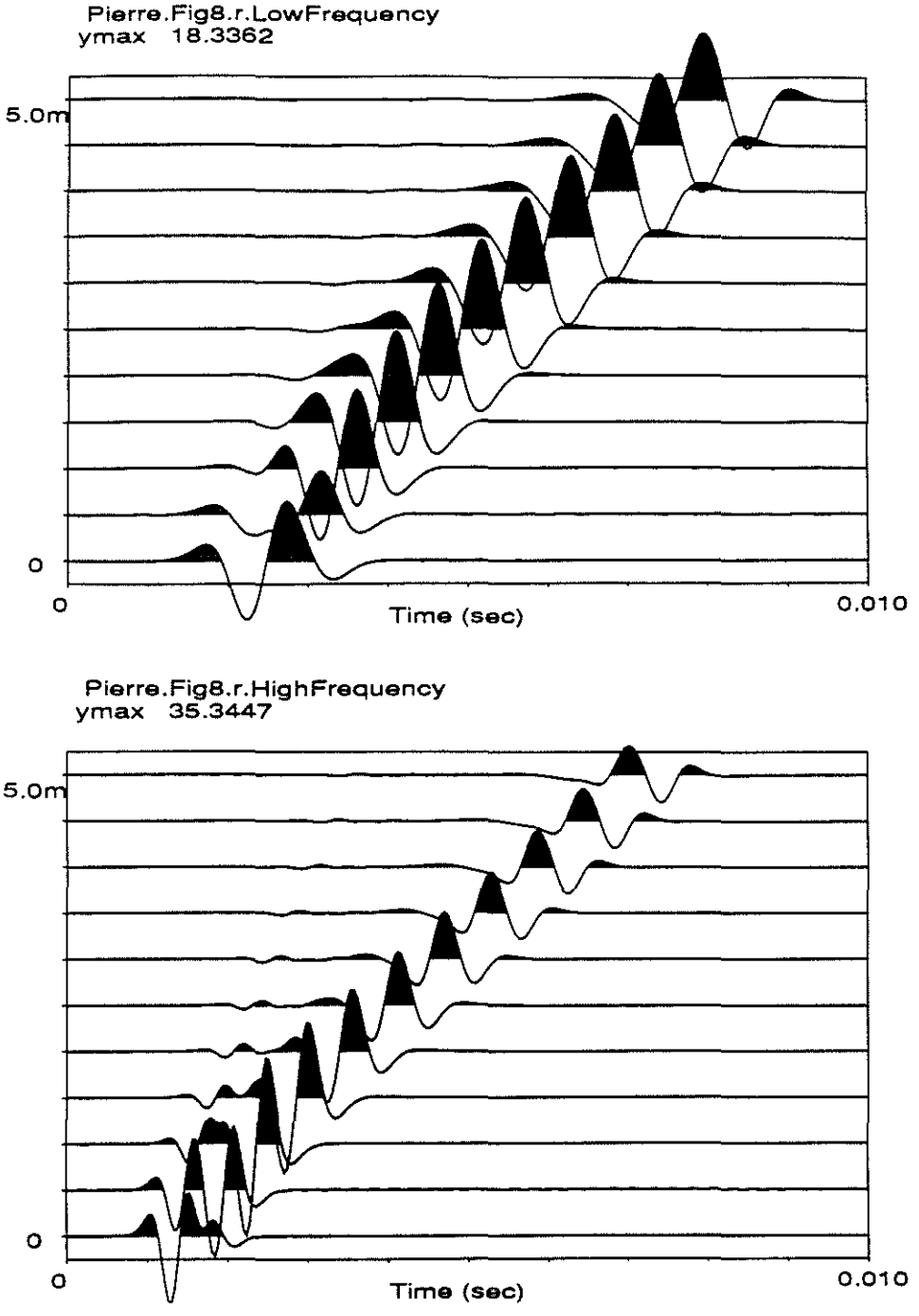


Figure 13: This figure shows a comparison of waveforms for varying source frequency at a distance of 5 m. Top shows radial component of a source in a fluid-filled borehole surrounded by Pierre shale with a center frequency of 750 hz and bottom for 1500 Hz.

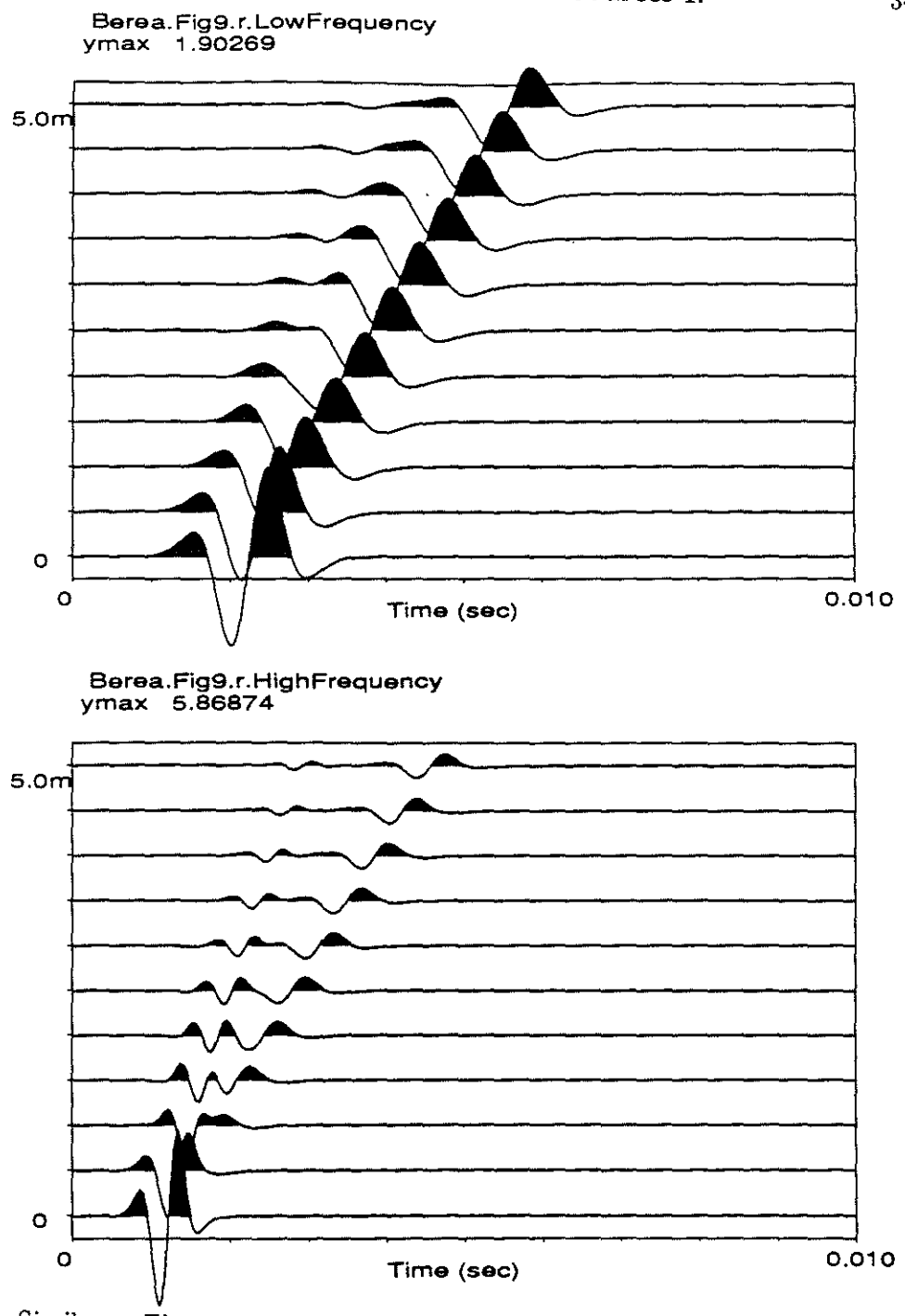


Figure 14: Similar to Figure 13, this figure shows the variation in waveform character and amplitude due to variations in frequency of the wavelet and impulse response but for Berea sandstone instead of Pierre shale. Top 750 Hz, bottom 1500 Hz center frequency.

# Appendix A. DISCRETE WAVENUMBER TECHNIQUE

## Introduction

This appendix will describe evaluation of integrals using the discrete wavenumber technique. Fundamentally, the discrete wavenumber technique evaluates a Fourier transform over wavenumber by discretizing the integral and introducing a periodicity to the medium and sources. An analogy can be made to discretizing an integral and evaluating it by using Simpson's rule. However, by introducing a periodicity into the medium, the sifting property of the Dirac delta and the periodicity of sinusoidal functions can be used to considerably reduce computation. That is the heart of the discrete wavenumber technique.

The discrete wavenumber technique evolved out of work by Rayleigh (1907) who studied periodic corrugated interfaces plus work by Aki and Larner (1970) who modelled irregularity in the Moho. Aki and Larner introduced a periodicity into the medium and also complex frequency to simplify calculation. Bouchon and Aki (1977) used the technique to calculate near field seismograms and compared the resulting seismograms favorably with analytical results for Lamb's problem. Bouchon and Aki also introduced the discrete wavenumber name to geophysics and showed how pre and post multiplication by a small factor $e^{i\omega_I t}$ in the frequency domain was advantageous to reduce aliasing. Bard and Bouchon (1980a,b) applied the technique to solve for displacement resulting from $Sh$ (1980a) and $P-Sv$ (1980b) waves incident on sediment filled valleys surrounded by basement. Bouchon (1981) showed the discrete wavenumber technique could be used to numerically evaluate Green's functions. Cheng and Toksöz (1981) were the first to utilize the technique in the borehole environment when they calculated synthetic seismograms from a source initiated in a borehole.

The discrete wavenumber technique has become a powerful technique for forward modelling. It has been applied to modelling of VSPs (Dietrich et al., 1984; Dietrich and Bouchon, 1985), calculation of synthetic seismograms in porous media (Schmitt et al., 1988), calculation of synthetic seismograms in radially layered media (Tubman, 1984; Tubman et al., 1984), and the calculations of synthetic seismograms in irregularly "layered" media (Campillo and Bouchon, 1985) where the discrete wavenumber technique was used in conjunction with the reflectivity technique (Kennett, 1983). Finally, a hybrid boundary-integral, discrete wavenumber technique has been developed for the calculating synthetics in media with irregular interfaces separating layers (Bouchon et al., 1989). The limitations of the Bouchon et al., results include $Sh$ (acoustic) wave propagation and two dimensional propagation.

As a side remark, White and Zechman (1968) did introduce a periodicity into the source and a periodicity in wavenumber. The only element of the discrete wavenumber technique they did not address was the important multiplication by the factor $e^{\omega_I t}$.

This work preceded that of even Aki and Larner (1970).

## Description of the Technique

This development will parallel the development in Bouchon and Aki (1977) but for cylindrical media. Begin with a double Fourier transform of a function $F(r,\theta,z,t)$ over wavenumber $k_z$ and frequency.

$$F(r,\theta,z,t) = \int_{-\infty}^{\infty}\int_{-\infty}^{\infty} f(r,\theta,k_z,\omega)e^{-ik_z z}e^{i\omega t}\,dk_z\,d\omega. \qquad (A-1)$$

We introduce a periodicity into the source by considering an infinite number of sources spaced a distance L apart along the $z$ axis. For the sake of brevity we will not display the integral over $\omega$. We integrate over this infinite number of sources and will call this new integral $G$

$$G(r,\theta,z,\omega) = \int_{-\infty}^{\infty} f(r,\theta,k_z,\omega)(\ldots e^{-ik_z(z-2L)}+e^{-ik_z(z-L)}+e^{-ik_z z}+e^{-ik_z(z+L)}+e^{-ik_z(z+2L)}+\ldots)dk.$$

$$G(r,\theta,z,\omega) = \int_{-\infty}^{\infty} f(r,\theta,k_z,\omega)e^{-ik_z z}\sum_{m=-\infty}^{\infty} e^{ik_z mL}dk_z. \qquad (A-2)$$

The summation term ($\sum e^{imk_zL}$) can be simplified by considering it as a Fourier series. We recognize the summation term as resembling a delta function. The calculation of the Fourier coefficients for a delta function proceeds as follows.

$$\sum_{m=-\infty}^{\infty} a_m e^{imk_z} = \delta(k_z) \qquad (A-3)$$

$$a_m = \frac{1}{2\pi}\int_0^{2\pi}\delta(k_z)e^{imk_z}dk_z. \qquad (A-4)$$

The sifting property of the delta function tells us that the right hand side integral equals $\frac{1}{2\pi}$

$$a_m = \frac{1}{2\pi}.$$

To determine the coefficients $a_m$ for our summation term we scale $k$ by $L$, so $k = kL$. The limits of integration are now from 0 to $2\pi L$ and $dk^{old} = Ldk^{new}$. We substitute the limits of integration and new differentials into Eq. A-4. The increase in range

of integration is irrelevant because the integral is evaluated by the sifting property exclusively at 0. Eq. A-4 becomes

$$a_m = \frac{1}{2\pi}\int_0^{2\pi L} L\delta(kL)e^{imkL}dk \qquad \text{(A-5)}$$
$$a_m = \frac{L}{2\pi}.$$

Now substituting the value of $a_m$ into the Fourier coefficient summation operator (Eq. A-3)

$$\sum_{m=-\infty}^{\infty} \frac{L}{2\pi} e^{imk_zL} = \delta(k_zL)$$

or equivalently

$$\sum_{m=-\infty}^{\infty} e^{imk_zL} = \frac{2\pi}{L}\delta(k_zL). \qquad \text{(A-6)}$$

The delta function in this case is periodic because of its dependence on the periodic $e^{imk_zL}$. The periodicity can be demonstrated by substituting values of $k_zL = 2\pi n$ where $n$ is any integer into the summation and showing that these new values of the exponential also satisfy the equality (Eq. A-6). Therefore, we can write

$$\sum_{m=-\infty}^{\infty} e^{imk_zL} = \frac{2\pi}{L}(\delta(k_zL))_{modulo\ 2\pi} \qquad \text{(A-7)}$$

where

$$\delta(k_zL)_{mod\ 2\pi} = 1 \quad k_z = \ldots \frac{-4\pi}{L}, \frac{-2\pi}{L}, 0, \frac{2\pi}{L}, \frac{4\pi}{L} \ldots$$

and zero otherwise. Therefore $\delta(k_zL)$ is in fact equal to $\frac{2\pi m}{L}$. Substituting Eq. A-7 into the integral Eq. A-2, we obtain the following

$$\int_{-\infty}^{\infty} f(k_z,\omega)e^{-ik_zz}\frac{2\pi}{L}(\delta(k_zL))_{mod\ 2\pi}dk_z = \frac{2\pi}{L}\sum_{n=-\infty}^{\infty} f(r,\theta,k_{zn},\omega)e^{-ik_{zn}z} \qquad \text{(A-8)}$$

where $k_{zn} = \frac{2\pi n}{L}$.

The function $F(r,\theta,z,t)$ is recovered from $G(r,\theta,z,t)$ by time windowing. The periodicity interval $L$ is chosen such that arrivals from fictitious sources will arrive after events of interest occur.

## Practical Considerations

A summation over an infinite number of wavenumbers is impossible and therefore in a computer algorithm some convergence criteria are applied. A typical criterion might be convergence until the value of the summand at one $n$ is only $\epsilon$ different from a previous $n$ and then evaluation stops.

It is very common to find that the kernel $f(r, \theta, k_{zn}, \omega)$ is either exclusively even or odd. If the kernel is even we can write

$$\frac{2\pi}{L} \sum_{n=0}^{\infty} \varepsilon_n f(r, \theta, k_{zn}, \omega) \cos(k_{zn} z) \qquad (A-9)$$

and if odd

$$-i\frac{2\pi}{L} \sum_{n=0}^{\infty} \varepsilon_n f(r, \theta, k_{zn}, \omega) \sin(k_{zn} z) \qquad (A-10)$$

where the $\varepsilon_n$ term is the well known Neumann's factor, $\varepsilon_0 = 1$, $\varepsilon_n = 2, n \neq 0$.

As explained in Bouchon and Aki (1977), in order to integrate across the real axis it is necessary to lift the singularities in $k_{zn}$ off the real axis slightly. This is done by introducing a small positive imaginary component to the frequency, remembering $k_{zn}$ is a function of $\omega$. The equation from Bouchon and Aki is

$$\omega = \omega_R - i\omega_I \qquad \text{with } w_I > 0 \qquad (A-11)$$

The effect of the imaginary part can be removed by post multiplication in the time domain of $e^{\omega_I t}$.

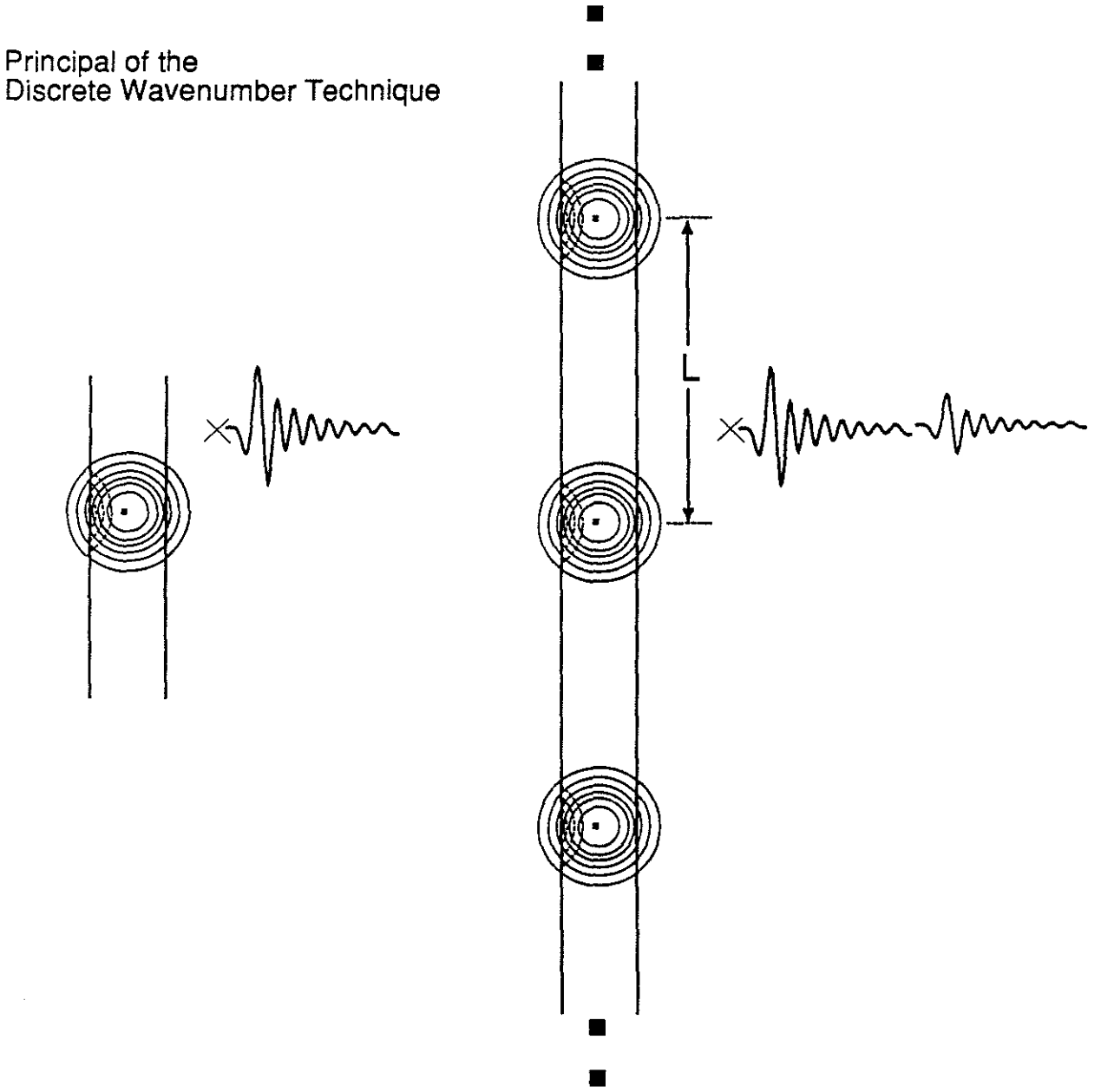


Figure A-1: Figure demonstrates the introduction of a periodicity into the source by replicating the source at distances spaced "L" apart. "L" is chosen so that arrivals from fictitious sources arrive outside of the time window of interest.

# Appendix B. PROGRAMMING CONSIDERATIONS

## Normalization

Normalization is an important aid in producing programs to calculate synthetic seismograms. By normalizing variables, different systems of units for length measurements, velocities and density measurements can be utilized. The particular strategy adopted throughout this paper when developing programs for it was to normalize all linear quantities by radius $a$ as the following diagram shows

$$\begin{aligned}
\Delta k_{zn}, dk_z &\rightarrow \frac{2\pi a}{z} \\
k_{zn} = \frac{2\pi n}{L} &\rightarrow \frac{2\pi n a}{L} \\
L &\rightarrow \frac{L}{a} \\
a &\rightarrow a \\
v_p, v_f, v_s &\rightarrow \frac{v_p}{a}, \frac{v_s}{a}, \frac{v_f}{a} \\
q_p, q_s &\rightarrow q_p, q_s \\
\rho &\rightarrow \rho \\
l, m, f &\rightarrow la, ma, fa \\
K_{\{0,1\}}(\{l,m,f\}a), I_{\{0,1\}}(\{l,m,f\}a) &\rightarrow K_{\{0,1\}}(\{l,m,f\}), I_{\{0,1\}}(\{l,m,f\}) \\
z &\rightarrow \frac{z}{a}
\end{aligned}$$

A question arises as to how this normalization applies to the calculation of our coefficients. Take the calculation of $g$, for instance, Eq. 105

$$g = \frac{f'\rho_b}{l'\rho_f}\left[\left(2\frac{\beta^2}{c^2}-1\right)^2 \frac{K_0(l'a)}{K_1(l'a)} - \left(\frac{2\beta^2 l'm'}{\omega^2}\right)\left[\frac{1}{m'a} + \frac{2\beta^2}{c^2}\frac{K_0(m'a)}{K_1(m'a)}\right]\right]. \qquad \text{(B-1)}$$

This can be written in normalized coordinates as

$$g = \frac{f'\rho_b}{l'\rho_f}\left[\left(2\frac{\beta^2}{c^2}-1\right)^2 \frac{K_0(l')}{K_1(l')} - \left(\frac{2\beta^2 l'm'}{\omega^2}\right)\left[\frac{1}{m'} + \frac{2\beta^2}{c^2}\frac{K_0(m')}{K_1(m')}\right]\right]. \qquad \text{(B-2)}$$

We can see that changes have occurred in the $\frac{1}{ma}$ term and in the argument for modified Bessel functions only. We now evaluate $A$ and $C$.

$$A = \frac{\frac{-2}{l'a}\left(\frac{2\beta^2}{c^2}-1\right)\frac{1}{K_1(l'a)}}{gI_1(f'a)+I_0(f'a)} \tag{B-3}$$

$$C = \frac{\frac{4i\beta^2}{\rho_b\omega ca}\frac{1}{K_1(m'a)}}{gI_1(f'a)+I_0(f'a)}.$$

We know that the denominator from Eq. B-1 has been properly normalized for both. So we rewrite the coefficients

$$A = \frac{\frac{-1}{l'}\left(\frac{2\beta^2}{c^2}-1\right)\frac{1}{K_1(l')}}{gI_1(f')+I_0(f')} \tag{B-4}$$

$$C = \frac{\frac{2i\beta^2 k_z}{\rho_b\omega c}\frac{1}{K_1(m')}}{gI_1(f')+I_0(f')}.$$

In the $C$ term, the factor $\rho_b$ has been introduced and it is not compensated by a $\rho_f$ as in the $g$ term. Therefore, we will have to input $\rho_b$ and also $\rho_f$ in a consistent set of units throughout our calculations. The units of $\frac{kg}{m_3}$ were used in the programs we developed. Now inserting the value of these coefficients into our discrete wavenumber summation,

$$U_r = \frac{2\pi}{L}\sum_{-\infty}^{\infty}(-Al'K_1(l'r)+ik_{zn}CK_1(m'r))e^{-ik_{zn}z} \tag{B-5}$$

$$U_z = \frac{2\pi}{L}\sum_{-\infty}^{\infty}(-ik_{zn}AK_0(l'r)-m'CK_0(m'r))e^{-ik_{zn}z}. \tag{B-6}$$

We can see that the $k_{zn}, l', m', L$ terms are different from their true values by the factor $a$ which cancels top and bottom.

Another simplification was adopted in the programming. The simplification was to let the user input the value of $L_{new} = \frac{2\pi}{L}$ instead of $L$ so that $k_z = \frac{L_{new}}{a}$ simplifying some computations.